(NASA CR-) OTS: $2.00

T-

PROTON DAMAGE IN SEMICONDUCTOR DEVICES

Final Report, 16 Apr. — 1 Nov. 1962

By D. M. Arnold, J. A. Baicker, H. Flicker, D. A. Gandolfo, J. R. Parker, et al, J. Vilms, and J. Vollmer

Apr. 1964

73 p refs

(NASA) Prepared under Contract No. NAS1-1654 by

RADIO CORPORATION OF AMERICA

Camden, New Jersey

NATIONAL AERONAUTICS AND SPACE ADMINISTRATION

For sale by the Office of Technical Services, Department of Commerce,
Washington, D.C. 20230 -- Price $2.00

FOREWORD

The Radio Corporation of America submits this final report in fulfillment of National Aeronautics and Space Administration Contract Number NAS1-1654. The work reported herein has been carried out by the Applied Research Group of RCA's Defense Electronic Products with significant contributions from the RCA David Sarnoff Research Center. This report covers the work performed during the contract period beginning 16 April 1962 and ending 1 November 1962.

INTRODUCTION

It has become important to understand and be able to predict the extent of proton damage to semiconductor devices. This requires an understanding of the fundamental physical processes involved. Accordingly, the objective of the study reported here is to interpret the observed changes in electrical characteristics of transistors in terms of fundamental changes in the semiconductor crystal structure. Once understanding is thus achieved, the prediction of the effects of protons on transistors will be possible. The displacement of atoms from equilibrium lattice sites, the introduction of impurities by means of nuclear transmutation and electron excitation are the effects considered; but interest is mainly centered on permanent changes in device characteristics caused by displacements.

The displacement production rate in silicon is calculated in Section I as a function of proton energy. Nuclear transmutations are also discussed here. In Section II the displacement production rate resulting from a neutron bombardment is calculated. In Section III the effect of lattice displacements on minority carrier lifetime, the most sensitive electrical property of semiconductors is discussed. The relationship between the lifetime damage constants which characterize proton and neutron bombardments is also considered. In Section IV attention is turned to the transistor itself, the analytical model of the device and the response to radiation in terms of this model. In this section use is made of neutron irradiation data in conjunction with the proton and neutron displacement production rates and the effect of proton bombardment is predicted. Reasonable agreement with experiment is obtained. Section V discusses the radiation environment of near space, namely the inner Van Allen belt and the expected life of selected transistors in this environment. Ionization and electron excitation effects are considered in Section VI.

TABLE OF CONTENTS

TABLE OF CONTENTS (Continued)

LIST OF ILLUSTRATIONS

LIST OF ILLUSTRATIONS (Continued)

SECTION I

PROTON INDUCED LATTICE DISPLACEMENTS

INTRODUCTION

The problem of calculating the damage which is produced by bombarding silicon with energetic protons may be conveniently divided into three parts. The first part deals with the primary interaction between the incident proton and a silicon atom in a crystal lattice. This interaction may be any of a number of possibilities, including elastic scattering (both Coulomb and nuclear) and a variety of proton-induced nuclear reactions. At very low proton energies the Coulomb interaction is dominant, and Rutherford scattering is sufficient to explain the experimental results. At somewhat higher energies (the exact energy ranges will be discussed in some detail in the next section) it becomes necessary to include nuclear elastic scattering together with Rutherford scattering, and at still higher energies inelastic scattering and reaction processes must also be included.

The primary proton-silicon collision will produce a recoiling atom whose energy depends on the angle the recoil velocity makes with the incident proton direction and on the Q of the particular reaction involved, according to the well-known Q-equation[1]. For elastic scattering the recoil energy will have some value between zero and T_m, where

$$T_m = \frac{4\,(m/M)}{\left[1 + (m/M)\right]^2} E_{inc} \qquad (1)$$

where:

m is the proton mass,

M is the silicon mass,

E_{inc} is the incident proton energy in the lab system.

The actual recoil energy is given by

$$T = T_m \, \mathrm{Sin}^2 \frac{\theta}{2} \tag{2}$$

where θ is the angle through which the proton is deflected in the center-of-mass system.

In the discussion of the proton damage process, N_c, the number of collisions per centimeter of traversal of the crystal by the primary proton as a result of which sufficient recoil energy is imparted to produce one or more lattice displacements, will be computed.

$$N_c = \int_{E_d}^{T_m} n_{Si} \frac{d\sigma\,(T)}{d\Omega} \, dT \tag{3}$$

where:

n_{Si} is the density of silicon atoms in a crystal

E_d is the energy required to displace a lattice atom from its normal position, the cross-section $\frac{d\sigma}{d\Omega}$ is given as a function of the recoil energy T instead of the proton deflection angle θ.

N_d, the number of lattice displacements per centimeter along the track of the proton will then be computed. An energetic silicon atom that is displaced by a proton-silicon collison is capable of initiating a cascade of displacement-producing atomic collisions. The problem of calculating the number of secondary lattice displacements that will be produced by a primary recoil atom of specified energy has been studied by Kinchin and Pease[2], Seitz and Harrison[3] and Snyder and Neufeld.[4] If the average number of displacements per primary recoil of energy T is g (T), then

$$R_D = \int_{E_d}^{T_m} n_{Si} \, g\,(T) \frac{d\,\sigma\,(T)}{d\,\Omega} \, dT \tag{4}$$

Some of the implications and consequences of the Seitz-Harrison and Snyder-Neufeld models will be discussed elsewhere in this section.

The third part of the problem is concerned with the diffusion of the vacancies-interstitials from their initial locations. Early theoretical studies of radiation-induced lattice defects were based on the assumption that an intrinsic model should be used, i.e., the electronic energy levels of isolated vacancies and interstitials (James-Lark-Horovitz model). But modern experimental evidence is conclusive that vacancy-impurity combinations created as a result of irradiation are dominant damage centers in silicon. Free vacancies are created during bombardment, but they are unstable at room temperature. What role the interstitial atoms may play in the electrical damage process is still unknown.

Unfortunately for the sake of an absolute damage rate calculation this aspect of the problem is poorly understood at present.

The chief feature that any theoretical treatment of this problem must account for is the observed energy dependence of proton damage in silicon devices. Since there is a considerable amount of information on damage to silicon solar cells, reliance will be mainly placed on these data. The solar cell damage rate has been found to decrease approximately as 1/E at low bombarding energies (from 1.5 to 4.5 Mev). (This is what one would expect for Rutherford scattering and the experimental result is reassuring.) In the energy range from 8 Mev to 40 Mev the damage rate decreases slightly, but at a much slower rate than 1/E. Above 40 Mev the damage rate approaches 1/E again. The deviation from the low-energy 1/E curve represents a departure from Rutherford scattering which must be explained by some other process. The principal conclusion of the present study is that for energies below 100 Mev the deviation may be reasonably well accounted for by including nuclear elastic scattering as well as Coulomb elastic scattering.

THE PRIMARY PROTON-SILICON INTERACTION

It is assumed in all of the following discussion that a monoenergetic beam of protons is incident on a sample of silicon that is sufficiently thin that only a small energy loss to the beam can occur. At relatively low bombarding energies (below 10 Mev, roughly) there are two circumstances that are important: individual resonances in the compound-nucleus system may be important, and the entire scattering process is strongly dominated by the coulomb interaction between the proton and the charge of the silicon nucleus. In any practical radiation damage experiment, the assumption of a thin target is not valid on a scale comparable to the width of individual nuclear resonances, and hence it is logical to assume that the damage rate may be calculated by averaging over them. The overriding circumstance at low energies, then, is the dominance of Rutherford scattering. Since the Rutherford cross-section decreases rapidly with energy ($d\sigma/d\Omega$ varies as $1/E^2$), while the nuclear cross-section and inelastic cross-sections in general do not, there is some energy (to be determined either from the nuclear scattering data or from the available theoretical models of nuclear scattering or both) above which the non-Rutherford scattering processes will dominate.

There are two sources of information on the detailed shape of the elastic scattering cross-section of silicon, both of them indirect. The first source of information is the nuclear scattering experiments which have been performed over a number of years, and the second is an application of recent theoretical models of the proton-nuclear interaction. Although there is practically no data on proton scattering by silicon there is ample data on proton scattering by aluminium, which may be applied directly to silicon without major modification. The justification for being able to do so follows from the success of the nuclear optical model[5] in the energy range from 10 to 100 Mev. A number of excellent illustrations of the accuracy with which nuclear scattering may be predicted by the optical model are shown in Figures 1 and 2. For comparison purposes the cross-sections of aluminium and magnesium at 9.8 Mev are shown in Figure 3. There are evidently some differences, but they are not great, and one would expect them to become smaller as the energy increases and the optical model becomes better.

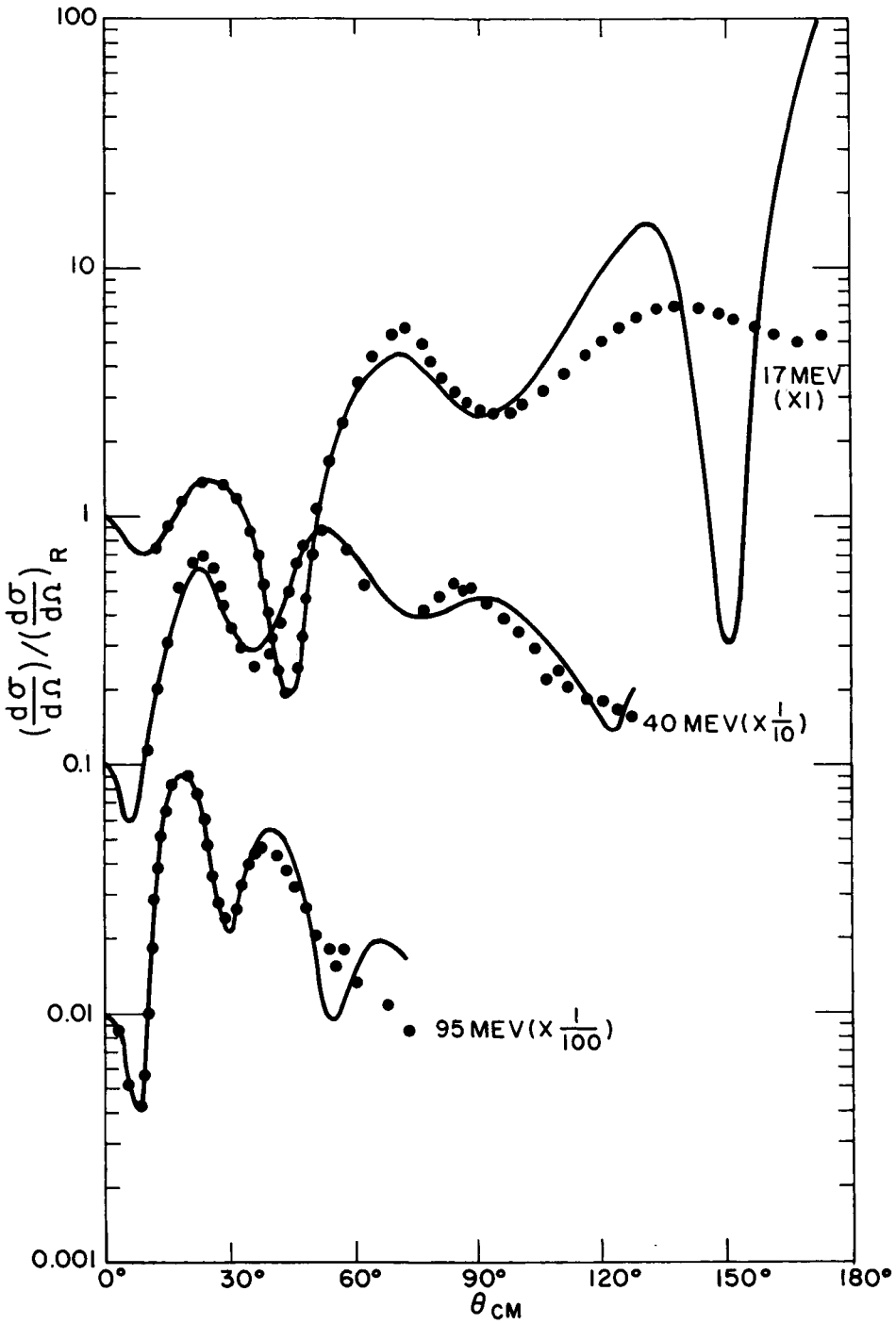

Figure 1. The ratio of the measured elastic cross-section $d\sigma/d\Omega$ to the Rutherford cross-section $(d\sigma/d\Omega)_r$ from protons scattered by aluminium at three different energies. The points are experimental, the solid curves are calculated using the optical model.

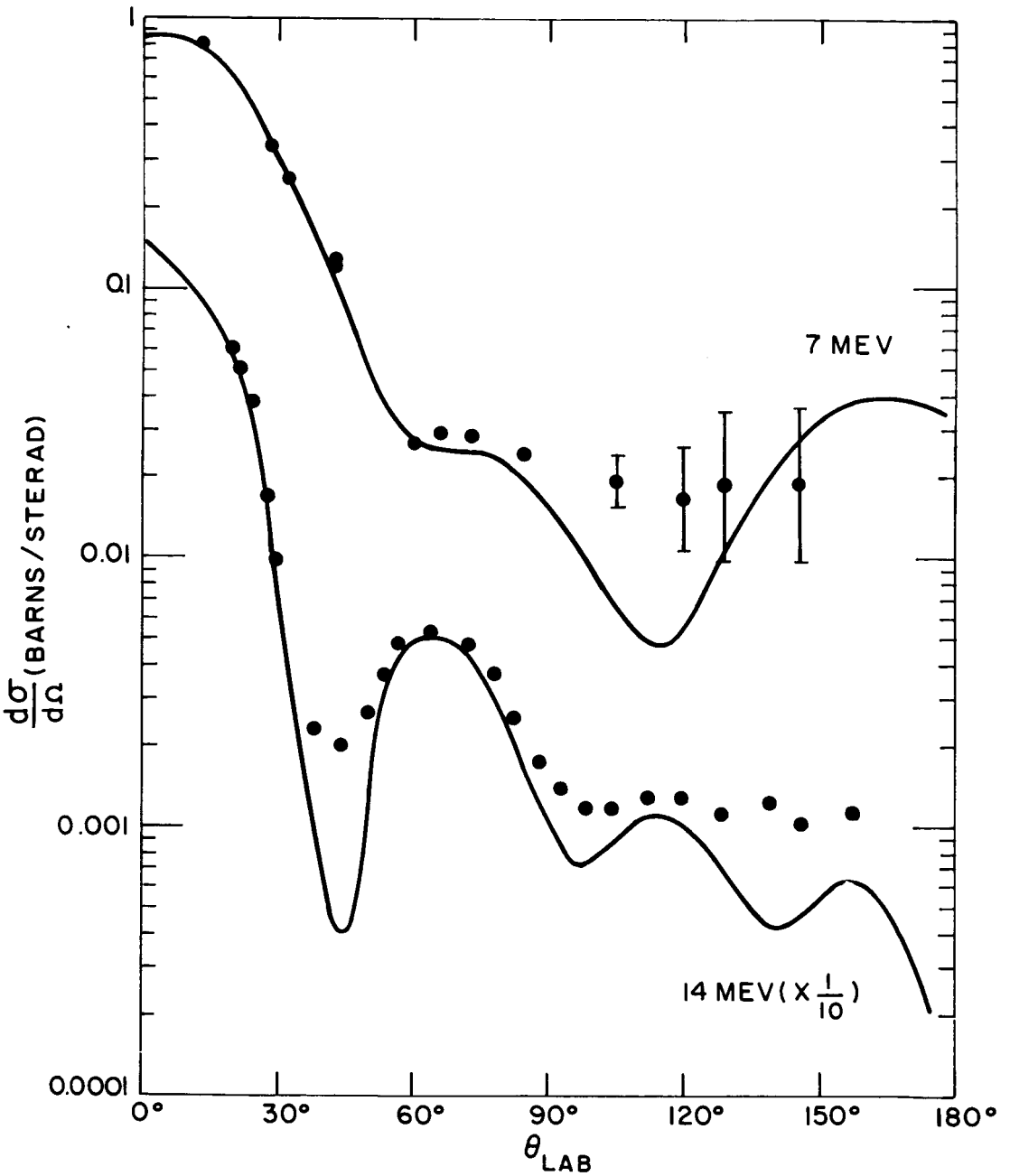

Figure 2. The elastic scattering cross-section for neutrons on aluminium at two energies. The points are experimental and the solid curves calculated using the optical model.

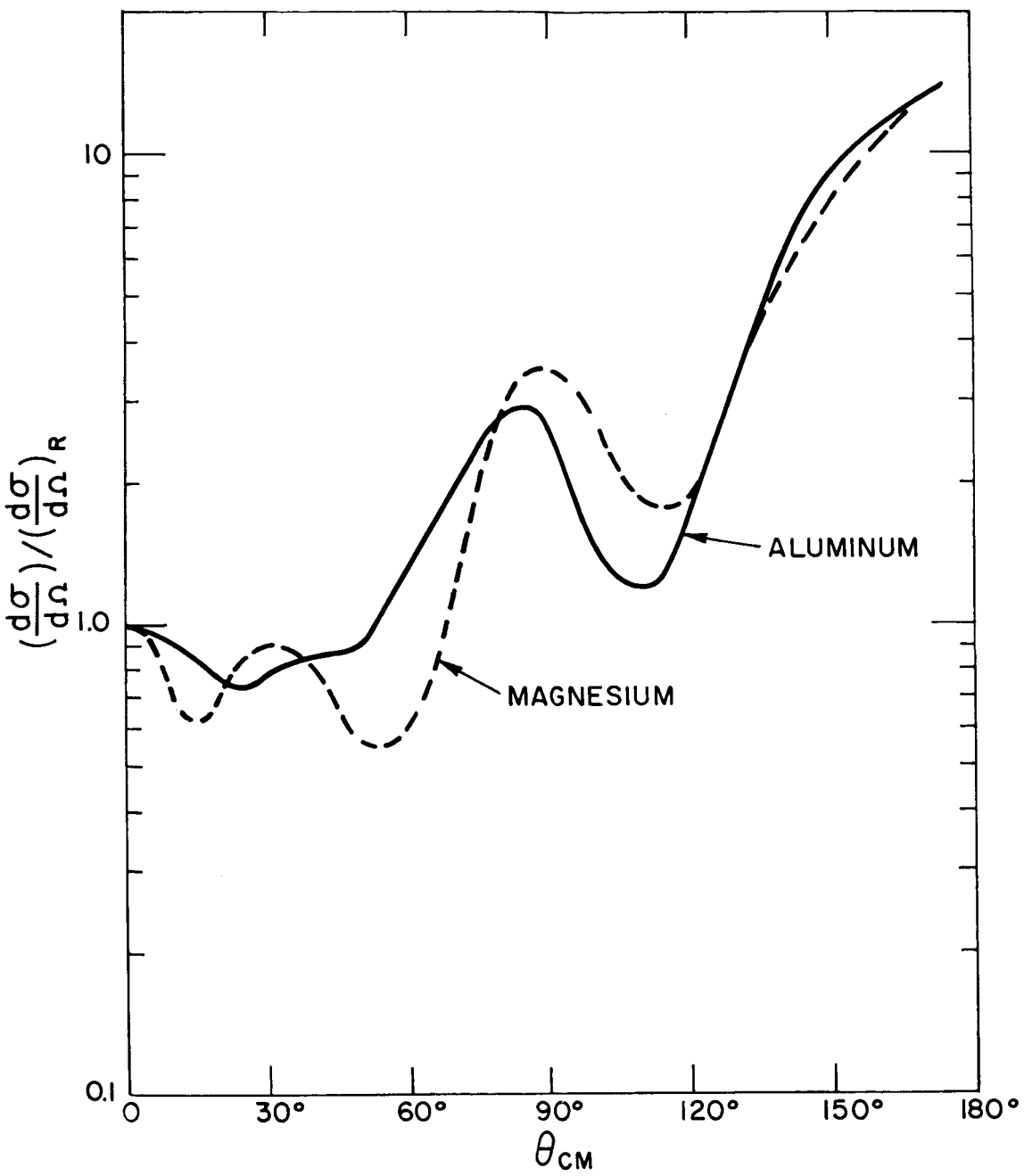

Figure 3. A comparison of the proton scattering cross-sections of magnesium and aluminium at approximately 10 Mev. The aluminium data is from ref. 7 and the magnesium data is from ref. 14.

Since the optical model is quite satisfactory in the intermediate energy region, and the parameters are very slowly varying functions of both energy and atomic weight of the nucleus one is amply justified in applying the aluminum scattering data to the silicon problem.

At sufficiently high energies there is also the likelihood that processes other than elastic scattering are important. At 100 Mev, for example, ordinary inelastic scattering, leaving the silicon nucleus in an excited state from which it decays by gamma emission, is roughly comparable to elastic scattering at all but small scattering angles. Equation (4) may be modified to include other than elastic processes.

$$R_D = \sum_j \int_{E_d}^{T_m} n_{Si}\, g(T)\, \frac{d\sigma_j(T)}{d\Omega}\, dT \qquad (5)$$

In order to evaluate equation (5) at the energies above 100 Mev which are being considered the differential cross sections for all important processes would have to be known. These would include, for example, (p,n), (p,d), (p,α), (p,T), (p,He^3), (p,2p), (p,pn), (p,2n), etc. Obviously such a complete collection of data does not exist. Nor is there a satisfactory theory by means of which approximate cross-sections could be calculated. Under these conditions the number of lattice displacements calculated from the elastic scattering cross-sections provides a lower limit for the actual damage rate. At 100 Mev this lower limit should not be more than a factor of roughly two below the actual damage rate, if the rather sparse inelastic scattering data is accepted.

Rutherford Scattering

The classical differential cross-section for Rutherford scattering is

$$\frac{d\sigma}{d\Omega} = \frac{\pi b^2}{16} \frac{1}{\mathrm{Sin}^4 \frac{\theta}{2}} \qquad (6)$$

where b is the classical distance of closest approach

$$b = \frac{2 \left| Z_1 Z_2 \right| \epsilon^2}{\mu v^2} \tag{7}$$

where:

$Z_1 \epsilon$ and $Z_2 \epsilon$ are the electrical charges of the incident particle and the target atom,

μ is the reduced mass of the incident particle, and

v is its velocity (lab system).

Seitz and Koehler[6] have given a concise discussion of the effect of electronic shielding of the nuclear charge. They point out that shielding effects are negligible provided $\theta >> \frac{b}{a}$ and $\frac{\lambda}{a}$ where λ is the proton's deBroglie wavelength ($\lambda = h/p$) and $a = \frac{a_o}{Z_2^{1/3}}$; p is the momentum of the proton and a_o is the radius of the Bohr orbit for hydrogen.

It is easy to show that for protons in the 10 to 100 Mev energy range this inequality is satisfied for all scattering angles sufficient to create one or more lattice displacements. Physically, this means that even for angular deflections of the proton beam as small as a few tenths of a degree the orbit of the proton passes well within the innermost electronic core of the lattice atoms.

Elastic Scattering Data in the 10 to 100 Mev Range

The elastic scattering cross-section for protons on aluminium has been measured at five different energies in the range of interest. These are listed in Table 1.

TABLE 1

Energy	References
9.8 Mev	7
17	8, 9
40	10, 11
95	12, 11
180	13

Inelastic Scattering

Since the inelastic scattering process is more distinctively characteristic of individual elements than elastic scattering it is not fully justified to draw general conclusions from a study of the behavior of atoms adjacent to silicon in the periodic table. Nevertheless, one is compelled to do so in the absence of such data on silicon. Matsuda et al[14] have measured both elastic and inelastic scattering by magnesium, and found that except at large scattering angles the elastic scattering is much larger than the inelastic. In silicon at 95 Mev the elastic and inelastic cross-sections are approximately equal (except at small scattering angles) and some correction to the calculated displacement density should be made. This will have the effect of increasing the number of displacements by less than a factor of two at 95 Mev.

PRODUCTION OF SECONDARY DISPLACEMENTS

This portion of the problem can be divided into parts. The first part is a determination of the interaction between a moving and a stationary silicon atom. A shielded coulomb potential of the form

$$V(r) = Z^2 \epsilon^2 \frac{e^{-r/a}}{r} \tag{8}$$

may be used to approximate the interaction, where $a = \frac{\lambda a_o}{Z^{1/3}}$, and λ is a number between 0.5 and 1.0.

For sufficiently low energies the collision between the moving and stationary silicon atoms involves no interpenetration of the electron clouds. The atoms repel each other with the sharply exponential potential $e^{-r/a}$. The scattering under these conditions is very nearly identical to hard-sphere scattering

$$\left(\frac{d\sigma}{d\Omega}\right)_{C.M.} = \frac{a^2}{4} \tag{9}$$

and the energy distributions of both the scattered atom and the recoiling atom are uniform from zero to the maximum possible recoil energy (neglecting the lattice binding the maximum recoil energy is equal to the incident atom's energy).

An upper limit to the energy at which the hard sphere approximation is valid is given by setting the distance of closest approach equal to a. Then

$$E_{\text{Hard Sphere}} \leq \frac{Z^2 \epsilon^2}{a} e^{-1} \tag{10}$$

For silicon $a \approx 10^{-9}$ cm and the energy must be $\leq 10^4$ ev for hard sphere scattering. For germanium the hard sphere approximation is good up to 7×10^4 ev.

At energies much greater than 10^4 ev the silicon-silicon scattering approaches Rutherford, the non-isotropic character of which would ordinarily complicate the computational problem if it were not for (1) the linearity of the cascade process once the energy drops to the hard-sphere range and (2) the near conservation of energy during the first part of the cascade. There is an additional complication at high energies. At energies above roughly 30 kev in silicon the recoiling atom is capable of producing ionization as well as lattice displacements, and at energies very far above 30 kev the ionization process will dominate. The transition from predominantly displacement production to predominantly ionization as the energy loss mechanism for the moving silicon atom occurs gradually and is not accurately known. In the next part of this section, dealing with the results of the calculations, the transition energy will be handled as a variational parameter, with the simplifying assumption that below the transition energy all energy loss is by atomic collisions, and above the transition energy all energy loss is by ionization.

The second part of the secondary displacement problem is a statistical analysis of the cascade process, which begins with a single silicon atom of energy T and terminates with N displaced silicon atoms each having energy less than E_d. The method of solution published originally by Snyder and Neufeld and used in the present

study is based on the following theorem of mathematical statistics. If N and Y are random variables, and the expectation value of N is $\epsilon [N]$, then

$$\epsilon [N] = \epsilon \left[\epsilon [N/Y] \right] \tag{11}$$

In the displacement cascade process, the number of displaced atoms N produced by the single primary atom of energy T, given that it will have an energy T_1 after the first collision, is equal to $N_1 + N_2$, where N_1 and N_2 are the numbers of displaced atoms produced after the first collision by cascades started by the original primary atom and the one it displaced, respectively. By observing that the statistics which determine N (or N_1 or N_2) are dependent only on T (or T_1 or T_2), it is possible to show that

$$\begin{aligned} g(x) &= \epsilon [N, x] = \epsilon \left[\epsilon \left[N_1, x_1 \right] + \epsilon \left[N_2, x_2 \right] \right] \\ &= \epsilon \left[g(x_1) + g(x_2) \right] \end{aligned} \tag{12}$$

where the notation N, x is employed to state explicitly the energy $x = T/E_d$ of the atom which starts the cascade that produces N displacements, and $(x_1 + x_2) = (x - 1)$. This can be rewritten

$$\begin{aligned} g(x) &= \epsilon \left[g(x_1) + g(x - x_1 - 1) \right] \\ &= \int \left[g(x_1) + g(x - x_1 - 1) \right] P(x_1)\, dx_1 \end{aligned} \tag{13}$$

For free hard-sphere scattering (Seitz-Harrison) $P(x_1) = 1/x$. Equation (13) can then be solved with the boundary conditions that for $x \leq 1$, $g(x) = 1$. The solution is

$$\begin{aligned} &g(x) = 1 && x \leq 1 && \text{(a)} \\ &g(x) = 1 + \log x && 1 \leq x \leq 2 && \text{(b)} \\ &g(x) \rightarrow 0.56\ (1 + x) && x >> 2 && \text{(c)} \end{aligned} \tag{14}$$

In the Seitz-Harrison model the silicon-silicon collision is treated as though it were in free space. The effect of the lattice is introduced by specifying that if the recoiling atom has an energy greater than the lattice binding energy ($\sim$13 ev in silicon) it has a unity probability of being displaced from its lattice site. This assumption is almost certainly too crude, but a more accurate representation including the functional dependence of escape probability on recoil energy would include additional parameters with which to fit experimental results. Since there is insufficient data in the present case to determine the extra parameters the simple step function will be used here.

The Snyder-Neufeld model includes the possibility of replacement collisions, in which the struck atom escapes while the incident silicon atom is trapped in its place. In their review article Seitz and Koehler give a plausible rationalization for ignoring this possibility, and in any event its inclusion does not alter the results very greatly. Thus

$$\begin{aligned} g(x) &= 1 && x \leq 2 && \text{(a)} \\ g(x) &\rightarrow 0.35\,x && x >> 2 && \text{(b)} \end{aligned} \qquad (15)$$

Both the Seitz-Harrison and Snyder-Neufeld models suffer from the disadvantage that the scattered and the recoiling silicon atoms are distinguishable after the collision has occurred. This disadvantage is more aesthetic than real in view of the crude nature of the basic assumptions of both models, but in order to explore the effect of eliminating this feature a modified treatment of the problem has been made. In this treatment the incident silicon atom is assumed to move into the same potential well in which the stationary atom is bound. (This may not be unreasonable provided the silicon-silicon interaction range is short compared with the lattice forces.) The silicon-silicon collision is then assumed to occur as though the lattice were absent (and it should be noted that in the classical free-space collision of identical particles the two are indistinguishable after the collision) and the incident energy is $E_{inc} + E_d$. Both silicon atoms must then have an energy greater than E_d in order to escape, and in so doing they each loose E_d. The solution to equation (13) in this case is

$$g(x) = 1 \qquad x \leq 1 \qquad \text{(a)}$$

$$g(x) = 1 + \log \frac{1 + x}{2} \qquad 1 \leq x \leq 2 \qquad \text{(b)} \qquad (16)$$

$$g(x) \rightarrow 0.47\ (1 + x) \qquad x >> 2 \qquad \text{(c)}$$

The three solutions given in equations 14-16 are shown in Figure 4. The present results are intermediate between the previous two, and in any event there is no great difference among the three.

THE CREATION OF ELECTRICAL DEFECTS

The process of diffusion of the vacancies (and perhaps interstitials) away from the point at which they were produced and their subsequent affiliation with crystal impurities, for example, to form electrically active centers is of critical importance to the radiation damage problem but is at present very poorly understood. Beginning with early experimental work which located the damage centers accurately within the bandgap, and culminating in the recent spin-resonance studies by Bemski[15] and by Watkins et al[16], several of the radiation defects have been identified in terms of chemical and physical configuration as well as electrical properties in the crystal. These include the A-center (an interstitial oxygen atom plus a vacancy), the E-center (a phosphorus donor atom plus a vacancy) and the C- and J-centers (different states of the di-vacancy). These are only a fraction of the important electrical centers, however, and even these differ greatly in their production rates under identical bombardment of ostensibly identical crystals. There appear to be many competing processes for the vacancies, some of which result in unimportant neutral centers and some producing important electrically "active" centers. As a consequence of this state of affairs it is impossible to predict by means of the sort of calculation outlined here what the absolute electrical defect density will be. Nor is it possible to account for the fluctuations that are observed from crystal to crystal. If the distribution in number of total displacements produced by the primary proton-silicon collision does not change too radically as a function of proton energy, however, a

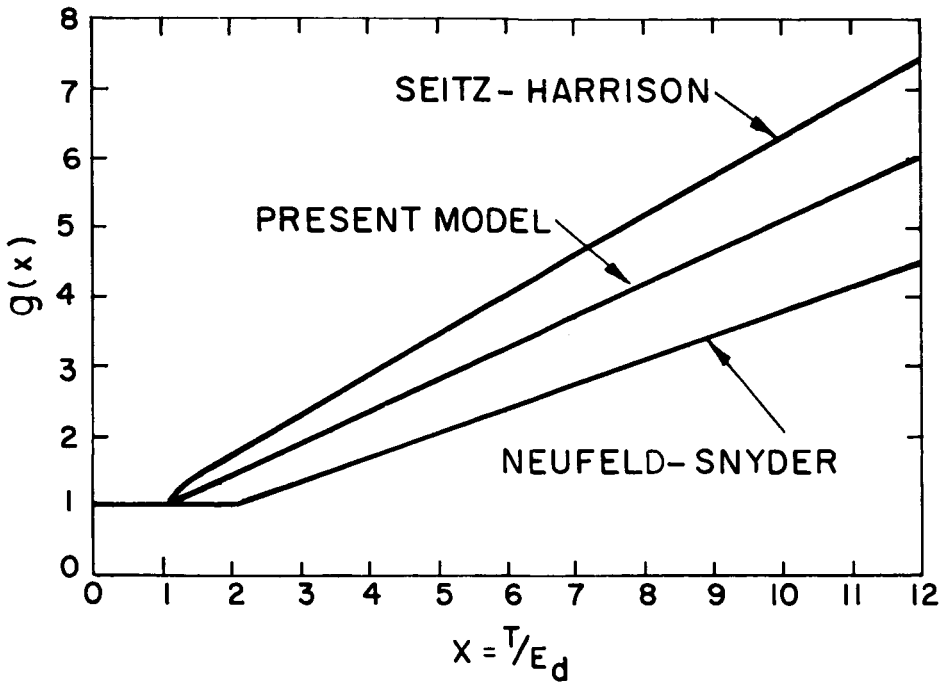

Figure 4. The average number of lattice displacements g (x) produced by a recoiling atom of energy $x = T/E_d$.

calculation of the total number of displacements such as described above will give a reasonable representation of the relative rate of introduction of electrical defects as a function of proton energy, averaged over many crystals. There is an implication in this step that all displacements are equally effective in producing electrical defects. Based on spin resonance studies as well as on other evidence that proton and electron bombardment produce different species of defect this assumption is not completely correct. It will still be a useful and reasonable approximation, however, provided the complex multiple vacancy-interstitial defects that are produced by proton irradiation are more effective as recombination centers, for example, than the single-vacancy defects produced by electron bombardment.

DISCUSSION

The displacement production rates have been calculated using the elastic scattering cross-sections at the five proton energies listed in Table 1. In the first approximation it was assumed that ionization effects by the recoiling silicon atoms were neglibible. The effect of this assumption was also investigated. Four different threshold energies for ionization were considered: 13.5, 27, 100 and 200 kev. It was assumed that below the threshold energy all energy loss occurred by atomic collisions, and above the threshold all energy loss was by ionization.

The results of the first calculations, in which ionization was neglected, are compared with the solar cell damage data in Figure 5. The points shown at 1.5 and 4.5 Mev were computed from the Rutherford cross-section, and the results at the five energies for which proton-aluminium scattering was used are as indicated. Considering the crudeness of the physical models that have been employed, the agreement between the calculations and the solar cell damage data is quite acceptable. Furthermore, if one were able to add the inelastic and higher-order processes the agreement at the high energy end would be improved.

Similar displacement versus energy curves for the four ionization thresholds listed above are shown in Figure 6. The displacement production rate is in reasonably good agreement with the damage data provided the effective ionization energy is $\geq$ 200 kev. There is very little direct experimental evidence which bears on this point, and future work might profitably be done on the subject.

To summarize the results of this Section, Rutherford scattering is sufficient to account for the observed proton damage only for bombarding energies below $\sim$8 Mev. From roughly 10 Mev to 50 Mev the results may be fairly well explained using Rutherford plus nuclear elastic scattering, and for energies above $\sim$100 Mev it is necessary to include inelastic scattering and perhaps other higher-order processes.

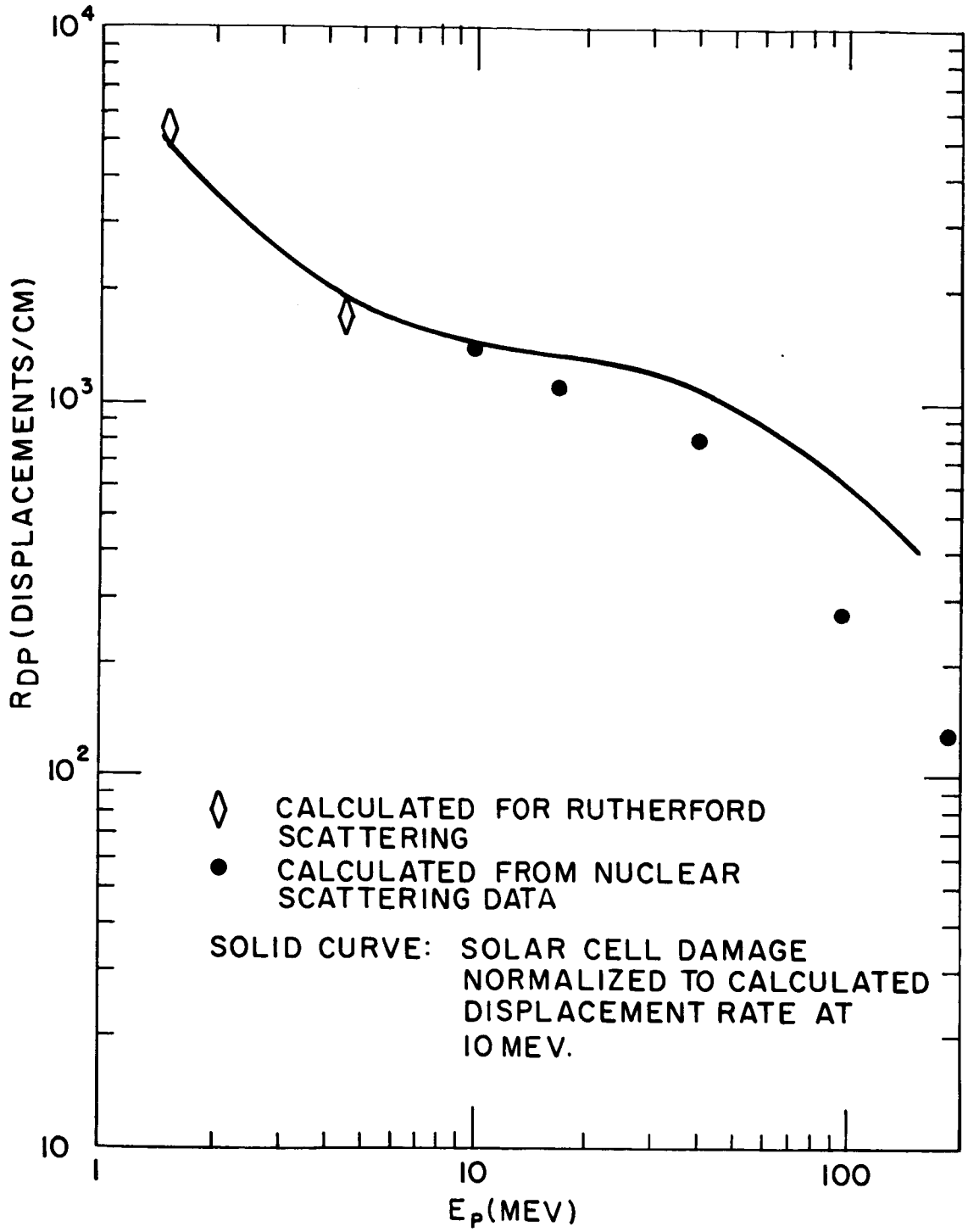

Figure 5. The number of lattice displacements R_{DP}, per centimeter along the track of an incident proton of energy E_p. Ionization effects by the primary recoiling silicon atom have been neglected.

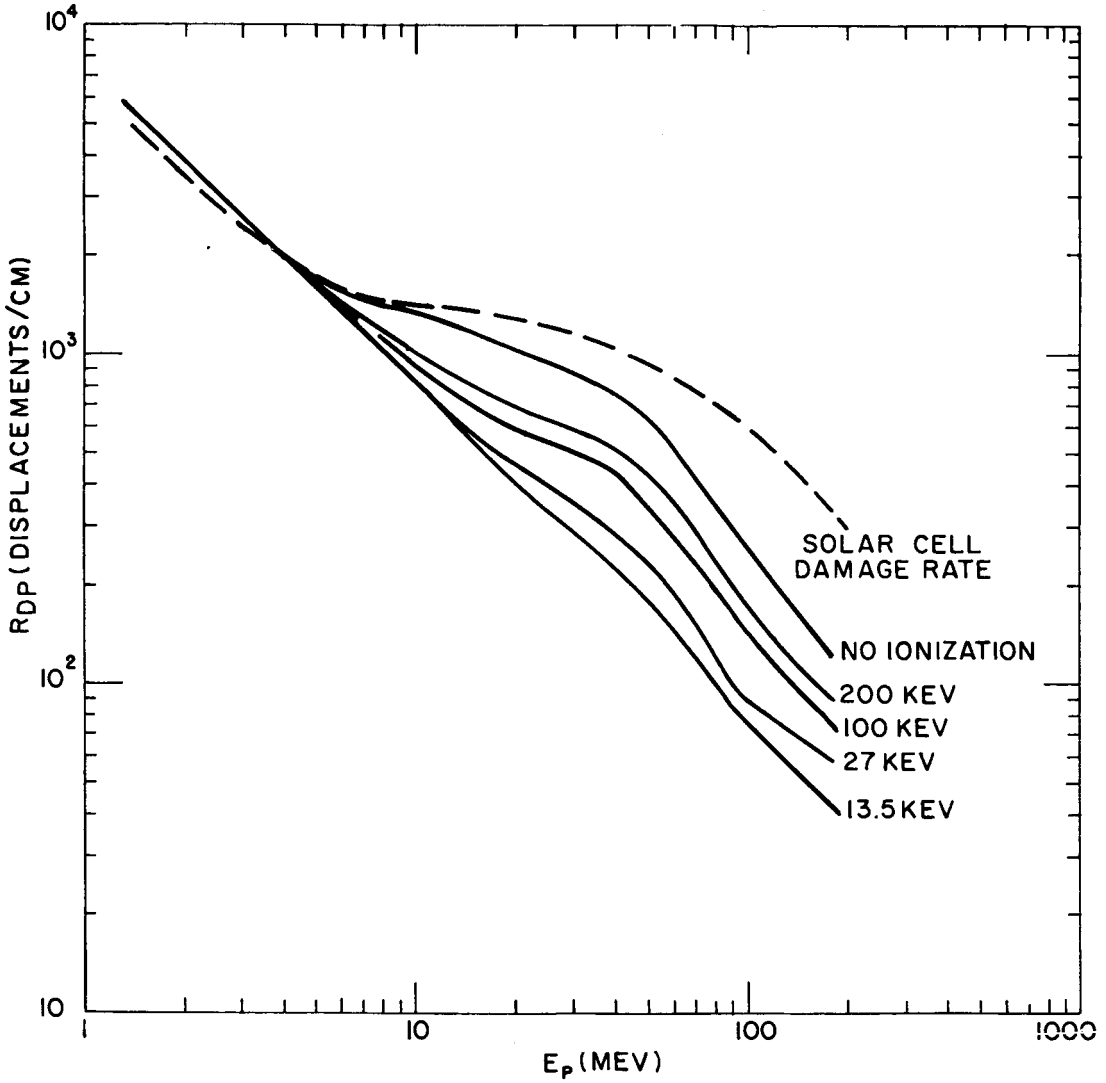

Figure 6. The number of lattice displacements along the incident proton track assuming various threshold energies above which electronic excitation is the principal energy loss mechanism for a recoiling silicon atom.

TRANSMUTATIONS

The possibility that nuclear transmutations might be significant in proton irradiation has been considered in some detail. Without presenting an extensive treatment of the theoretical and experimental information that is available on the subject it is possible to show by a fairly simple argument that transmutation products are indeed unimportant in the proton damage process. The total reaction cross section (which includes compound-elastic scattering as well as inelastic scattering and reactions at low energies) will tend to increase with proton energy at low energies, and will approach the geometrical cross section of silicon at high energies. This cross section may be used as an upper limit to the true cross section at any energy. Therefore

$$\sigma = \pi r^2 \tag{17}$$

where

$$r = A^{1/3} (1.4 \times 10^{-13} \text{ cm.}) \approx 4 \times 10^{-13} \text{ cm.}$$

Using this value, $\sigma = 5 \times 10^{-25} \text{ cm}^2$.

If the most pessimistic assumption is made, for example, that all of the reaction products are effective recombination centers, then the number per cm along the track of the proton in the crystal can be computed by

$$N_{trans} = n_{Si}\sigma = .025 \text{ cm}^{-1} \tag{18}$$

This number must be compared with the number of recombination centers resulting from the lattice displacements produced by the bombardment, which according to the best estimates is $\geq .02\ R_{DP}$. This number can be estimated from Figure 6. At 4 Mev the number of recombination centers produced by elastic scattering is 40 per cm, and at 180 Mev the number is 2 per cm. Even at the higher energy the number of transmutation-produced recombination centers is nearly a factor of 100 lower than the number produced by elastic scattering.

One may conclude, therefore that the final transmutation products are not important in proton bombardment in this energy range. This does not mean that the general class of inelastic processes may be neglected, however. Any recoiling atom having high kinetic energy will produce a high concentration of lattice displacements as it traverses the crystal, and previous comparison of the numbers produced by elastic scattering with the available damage data suggests strongly that such processes become important at high energies.

SECTION II

NEUTRON INDUCED LATTICE DISPLACEMENTS

INTRODUCTION

This phase of the problem differs slightly from that treated in the previous section inasmuch as the neutron is uncharged and one need consider only elastic nuclear scattering. Further, the interest here is in lower energies, 0 to 15 Mev, the energy range of neutrons produced by the nuclear reactors at which device irradiation experiments have been performed. Accordingly, the calculation of the damage rate, i.e., the number of defects per unit particle path is slightly modified. However, the same assumptions are made here regarding the validity of using aluminum elastic-scattering cross-section data in the absence of silicon data and regarding the defect cascade produced by a primary knock on.

NEUTRON DISPLACEMENT RATE

If the expression for the defect cascade function developed in the first part of this report (equation 16c) is substituted into equation 4 one obtains for the damage rate

$$R_{DN} = \frac{N_{DN}}{\varphi N} = \int_{E_D}^{T_m} n_{Si} \left[.47 \frac{T}{E_D}\right] \frac{d\sigma}{d\Omega}(T)\, dT \tag{19}$$

Recall now that the average energy of a primary knock-on is given by

$$\overline{T} = \frac{\int_T \frac{d\sigma}{d\Omega}(T)\, dT}{\int \frac{d\sigma}{d\Omega}(T)\, dT} = \frac{\int_T \frac{d\sigma}{d\Omega} dT}{\sigma_{Te}} \tag{20}$$

Therefore, equation 19 becomes

$$R_{DN} = \frac{.47\ n_{Si}}{E_D}\ \overline{T}\ \sigma_{Te} \tag{21}$$

where σ_{Te} is the total elastic scattering cross section. $\overline{T}$ has been calculated from equation 20 for neutron energies of 0, 4.1 and 14.1 Mev using differential and total elastic scattering cross sections for the neutron-aluminum interaction tabulated in BNL 400[49] and BNL 325[50]. Figure 7 shows a graph of the ratio $\overline{T}/T_m$ from 0 to 15 Mev. The linear interpolation between the 0 and 4.1 Mev points is justified by the fact that the shape of $\frac{d\sigma}{d\Omega}(T)$ varies slowly with neutron energy in this range. The shape of the curve above 4.1 Mev is of little importance since the total number of neutrons in this range is very much less than that between 0 and 4.1 Mev.

Binder[17] calculated $\overline{T}/T_m$ for neutrons in germanium in a manner similar to that outlined here. He used the decrease of this ratio with increasing neutron energy to interpret the results of the experiment of Ruby, et al[18] who found that 1.8,

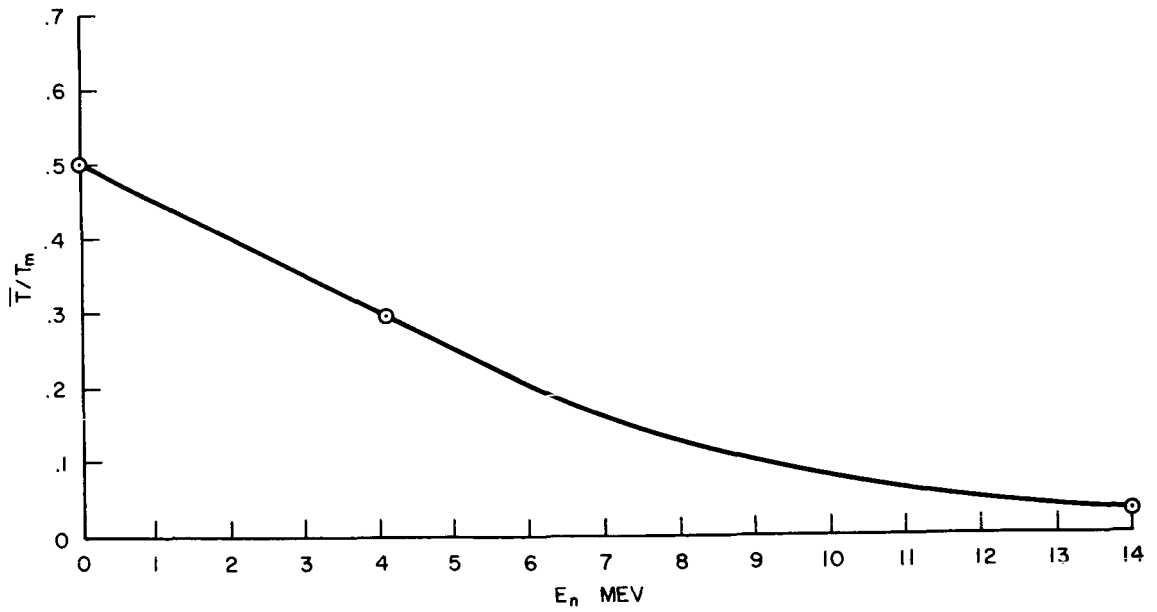

Figure 7. The Ratio of the Average Energy to the Maximum Energy Imparted to Recoil Silicon Atoms Displaced by Neutrons of Energy E_n

3.2 and 4.8 Mev neutrons produced the same electron removal rate in Ge. Binder showed that this correlated with a constant defect production rate over this energy range.

The value of σ_{Te} to be used in equation 21 may be obtained from Figure 8. This curve is a modified version of that shown for aluminum in BNL 325. Resonances have been smoothed over and the non-elastic component has been subtracted.

Using values of $\overline{T}$ and σ_{Te} from Figures 7 and 8 in equation 21, the damage rate R_{DN} at various neutron energies may be computed. Figure 9 shows R_{DN} from 0 to 10 Mev.

A weighted average value of the quantity R_{DN} over the energy spectrum of prompt fission neutrons is now determined. The fission spectrum is of interest because it is reasonably close to the energy spectrum of neturons from pulsed reactors. In a later section of this report device irradiation data obtained from experiments performed at these reactors is used in predicting the effects of proton irradiation

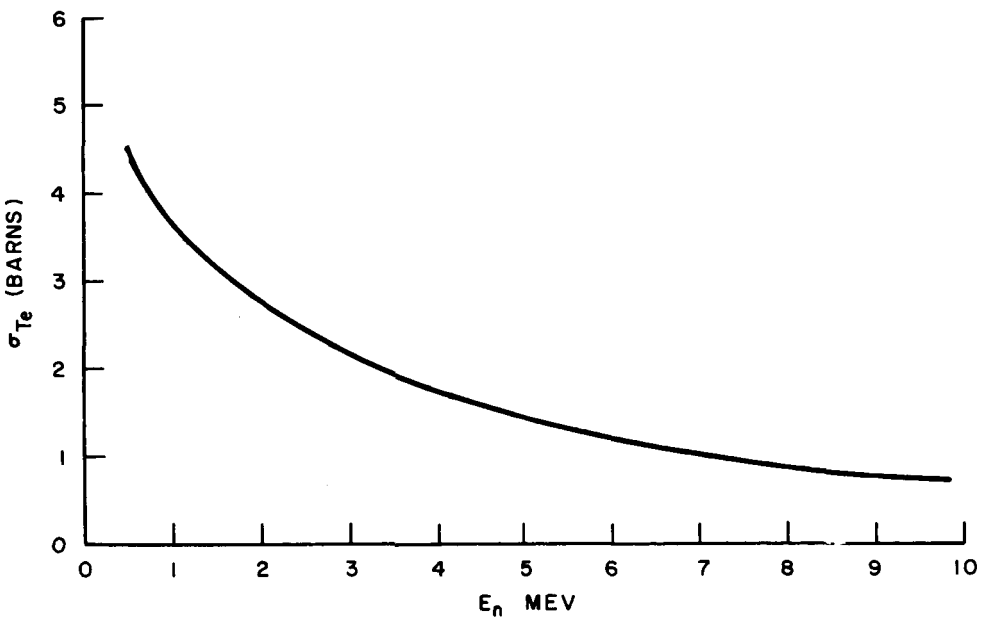

Figure 8. Total Elastic Scattering Cross Section, σ_{Te}, versus Neutron Energy, Neutrons on Aluminum

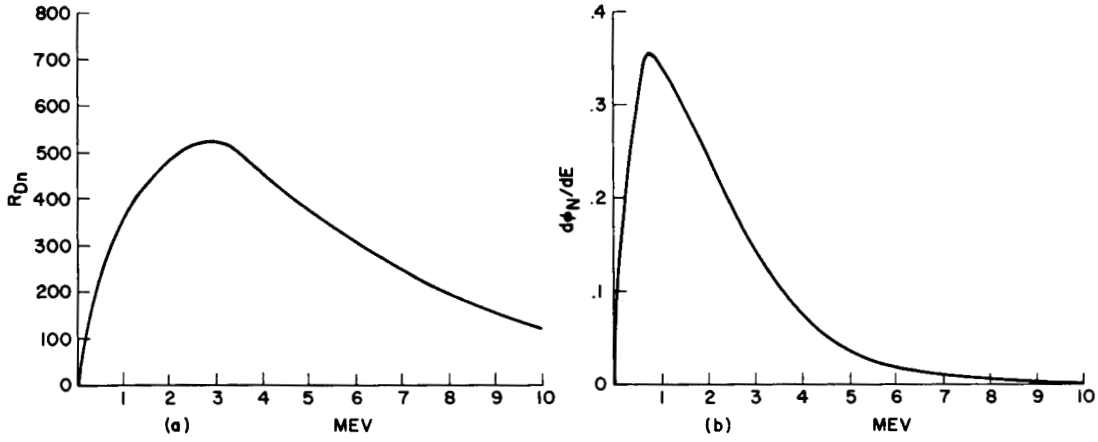

Figure 9. $R_{DN}(CM^{-1})$ and $d\varphi_N/dE$ versus E_n

on transistors. The advantages afforded by a well known energy spectrum of incident particles are obvious. The fission spectrum is given by Watt[19] by an expression of the form

$$\frac{d\varphi_N}{dE} = A \sinh \sqrt{2E} \quad -E \tag{22}$$

Table 2 has been constructed by Stephenson[20] with $d\varphi_N/dE$ normalized to one fission neutron. This table shows the relative number of neutrons in each energy interval.

The integral

$$\int R_{DN}(E) \frac{d\varphi_N}{dE} \, dE$$

has been evaluated numerically and the average value of R_D from 0 to 10 Mev is found to be $\overline{R}_{DN} = 376\ cm^{-1}$

$\overline{R}_{DN}$ for the pulsed TRIGA spectrum, as reported by DOFL[38], has also been calculated and found to have a value of $460\ cm^{-1}$.

These values of $\overline{R}_{DN}$ for the fission and TRIGA spectra will be used with R_{DP}, the displacement density per unit proton flux, to predict the effect of proton irradiation on transistors.

TABLE 2

RELATIVE NUMBER OF FISSION NEUTRONS

Energy Interval, Mev	Number based on one fission neutron
0 - 1	.308
1 - 2	.294
2 - 3	.186
3 - 4	.103
4 - 5	.055
5 - 6	.028
6 - 7	.0136
7 - 8	.00662
8 - 9	.00311
9 - 10	.00145

SECTION III

LIFETIME DAMAGE

INTRODUCTION

The minority carrier lifetime, τ, may be defined simply as the time during which a minority carrier (i.e., a hole injected into n-type material or an electron into p-type) exists as a free carrier before recombining with a majority carrier. Shockley and Read [21] developed a theory of recombination through the mechanism of the recombination center or trap which is associated with an imperfection in the semiconductor crystal. A recombination center consists essentially of an energy level (or levels) introduced by the lattice imperfection into the forbidden gap between the valence and conduction bands. In general, these energy levels are much closer to the center of the band gap than are the levels associated with the usual doping impurities. The fundamental physical processes occurring at the centers are electron capture, electron emission, hole capture and hole emission. The probability of the occurrence of these events governs the recombination process.

RECOMBINATION OF MINORITY CARRIERS

Shockley and Read derived an expression for the rate of recombination of minority carriers. This recombination rate is

$$U = \left\{ \frac{\sigma_n \sigma_p v_n v_p (pn - p_1 n_1)}{\sigma_n v_n (n + n_1) + \sigma_p v_p (p + p_1)} \right\} Nt \qquad (23)$$

Where: σ_n, σ_p are the cross sections for the capture of electrons and holes by the trap.

v_n, v_p are the mean thermal velocities of free electrons and holes.

n, p are the densities of electrons in the conduction band and holes in the valence band.

n_1, p_1 are the densities of electrons in the conduction band and holes in the valence band when the energy level of the trap is at the Fermi level.

N_t is the number of traps.

The minority carrier lifetime is inversely related to the recombination rate and therefore to the number of traps. Thus

$$\frac{1}{\tau} = CN_t \tag{24}$$

where C involves the capture cross sections, thermal velocities, energy levels and the Fermi level and may be considered to be independent of the number of traps as long as N_t is not large enough to perturb the Fermi level appreciably. It has been said that the traps are associated with lattice imperfections. The vacancies and interstitials created when energetic particles are incident on a semiconductor crystal constitute such imperfections, i.e., N_t is a function of φ. From equation 24 it is obvious that irradiation, by increasing N_t, causes τ to decrease.

Messenger and Spratt[22] have discussed the use of the Shockley - Read statistics in the problem of radiation induced changes in the minority carrier lifetime.

Loferski and Rappaport [23, 24, 25] determined experimentally that the lifetime of minority carriers in irradiated p-n junctions is inversely related to the integrated flux as follows

$$\frac{1}{\tau} = \frac{1}{\tau_o} + k\varphi \tag{25}$$

Where τ is the lifetime after an integrated flux, φ, of bombarding particles

τ_o is the initial lifetime

k is the lifetime damage constant.

Comparing equations 24 and 25, one sees that

$$\frac{\partial \left(\frac{1}{\tau}\right)}{\partial \varphi} = \text{constant} = K = C \frac{\partial N_t}{\partial \varphi} \tag{26}$$

It will now be assumed that $\frac{\partial N_t}{\partial \varphi}$ is directly proportional to the displacement production rate, R_{DP} or R_{DN}. That one may have confidence in this assumption is demonstrated by the good agreement between the calculated displacement production rate and the observed solar cell damage rate shown in Figure 5. Thus equation 26 may be written

$$\frac{\partial \left(\frac{1}{\tau}\right)}{\partial \varphi_N} = K_N = C'_n R_{DN}; \frac{\partial \left(\frac{1}{\tau}\right)}{\partial \varphi_p} = K_P = C'_p R_{DP} \tag{27}$$

Further, it will be assumed that the damage constants K_N and K_P are dependent on the irradiating particle only through the displacement production rates R_{DN} and R_{DP}. In other words it will be assumed that C'_n is equal to C'_p. This assumption permits one to eliminate C' between the two equations in (27) and obtain

$$K_P = \frac{K_N}{R_{DN}} R_{DP} \tag{28}$$

Thus, the lifetime damage constant for use with protons is given in terms of a lifetime damage constant obtained from neutron irradiation data and the displacement production rates for the two particles.

A rather large assumption was made above when it was stated that the damage constants depend on the particle types only through the defect production rates. This assumption ignores possible differences in energy levels and capture cross sections of the various defects. However, it has been shown previously that for proton energies above 10 Mev elastic nuclear scattering accounts for a significant

portion of the damage rate. Elastic nuclear scattering of protons occurs through the same mechanism as scattering of neutrons, i.e., through the interaction between the particle and the nuclear force field. This elastic nuclear scattering results in a much larger number of large deflection-angle scatterings than does Rutherford scattering. Large angle scattering of course means high energy primary knock-ons. Now if high energy protons produce primary knock-ons of energy comparable to those produced by neutrons, the resulting defect cluster might be expected to be similar. Therefore, the assumption regarding the damage constants is not an unreasonable one.

SECTION IV

ANALYTICAL MODEL OF THE TRANSISTOR

INTRODUCTION

The functional dependence of the electrical properties of semiconductor materials on radiation induced displacements has now been related to the type of radiation and the total radiation dosage for a given material. The allowable change in these electrical properties is entirely determined by the external electrical behavior of the semiconductor device. Hence, to determine an allowed radiation dosage one must establish the relationship between the material electrical properties and device electrical behavior.

Externally, the performance of a semiconductor device, such as a transistor can be described as a complex linear circuit in terms of any of six (6) sets of parameter matrices.[26] Each of these external parameters can in turn be related to the material electrical properties and the boundary conditions imposed by the device geometry and surface properties. The most commonly used parameter matrices are the Z, Y, A and H matrices. The possibilities are multiplied by three for transistors because the transistor allows a common connection, between input and output of the devices, of either the emitter, base or collector.

SELECTION OF PARAMETER TO BE STUDIED

For the study of radiation effects, the parameter or parameters which are critical to the circuit performance and sensitive to the radiation effects should be selected. For analysis and prediction of the radiation dependence of other parameters, or the

radiation dependence of the same parameter in a different radiation environment, the selected parameters should have clear and explicit relations to the device internal parameters, i.e., the material electrical properties, the geometry and the dimensions. A further requirement of this particular study is that there exist data on the variation of the selected parameter under neutron irradiation.

The H parameters appear to be peculiarly adapted to the physical characteristics of transistors.[27] Of these, the parameter which meets all of the above requirements is the common emitter forward current gain β.

In addition, β and its variation with frequency is the principal parameter which is common to both amplifier and switching circuits.

RELATION OF β TO SEMICONDUCTOR PHYSICS AND OPERATING CONDITIONS

There is currently under development a new "flux analysis" of transistors[28, 29] which should be very useful in accounting for radiation effects because it was evolved to account for the added carrier transport problem. It should also be useful in describing relations in transistor structures which have evolved from the junction transistors. This section shall, however, deal with all transistors in terms of the Webster[30] equation as though they were junction transistors. This relates the current gain to the internal parameters as follows

$$\frac{1}{\beta} = \text{surface recombination term} + \underset{\text{Lifetime Term}}{\text{Minority Carrier}} + \underset{\text{Efficiency Term}}{\text{Emitter}}$$

For pnp transistors this becomes

$$1/\beta = \frac{SWA_s}{D_p A_e}\, g(Z_p) + \left[\frac{W^2}{2D_p \tau_p} + \frac{\sigma_b W}{\sigma_e L_e}\right](1 + Z_p) \qquad (29)$$

and for npn's

$$1/\beta = \frac{SWA_s}{D_n A_e} g(Z_n) + \left[\frac{W}{2D_n \tau_n} + \frac{\sigma_b W}{\sigma_e L_e}\right] (1 + Z_n) \quad (30)$$

where:

S is the recombination velocity of surface carriers over the emitter-base surface.

W is the base width.

A_s is the surface area around emitter over which surface recombination of carriers occurs. The recombination current is

$$I_{SR} = S_e A_S p_{e'} \text{ or } S_e A_S n_e \quad (31)$$

for pnp's, and npn's respectively, where P_e (or n_e) is the hole or electron density at the emitter.

D_p and D_n are the diffusion constants for holes and electrons in the base region.

A_e is the cross sectional area of the conduction path which is approximately equal to the emitter area.

τ_p, τ_n are the minority carrier lifetimes in the base region.

σ_b, σ_e are the base and emitter conductivities.

The functions g (Z) and Z modulate the relative contributions of surface recombination, minority carrier lifetime, and emitter efficiency to produce the typical β versus I_E dependence shown in Figure 10.

The strong dependence of β on I_E clearly illustrates the necessity for eliminating emitter current dependence before assessing radiation damage data. The relative importance of surface versus bulk effects (conductivity and lifetime) will vary with

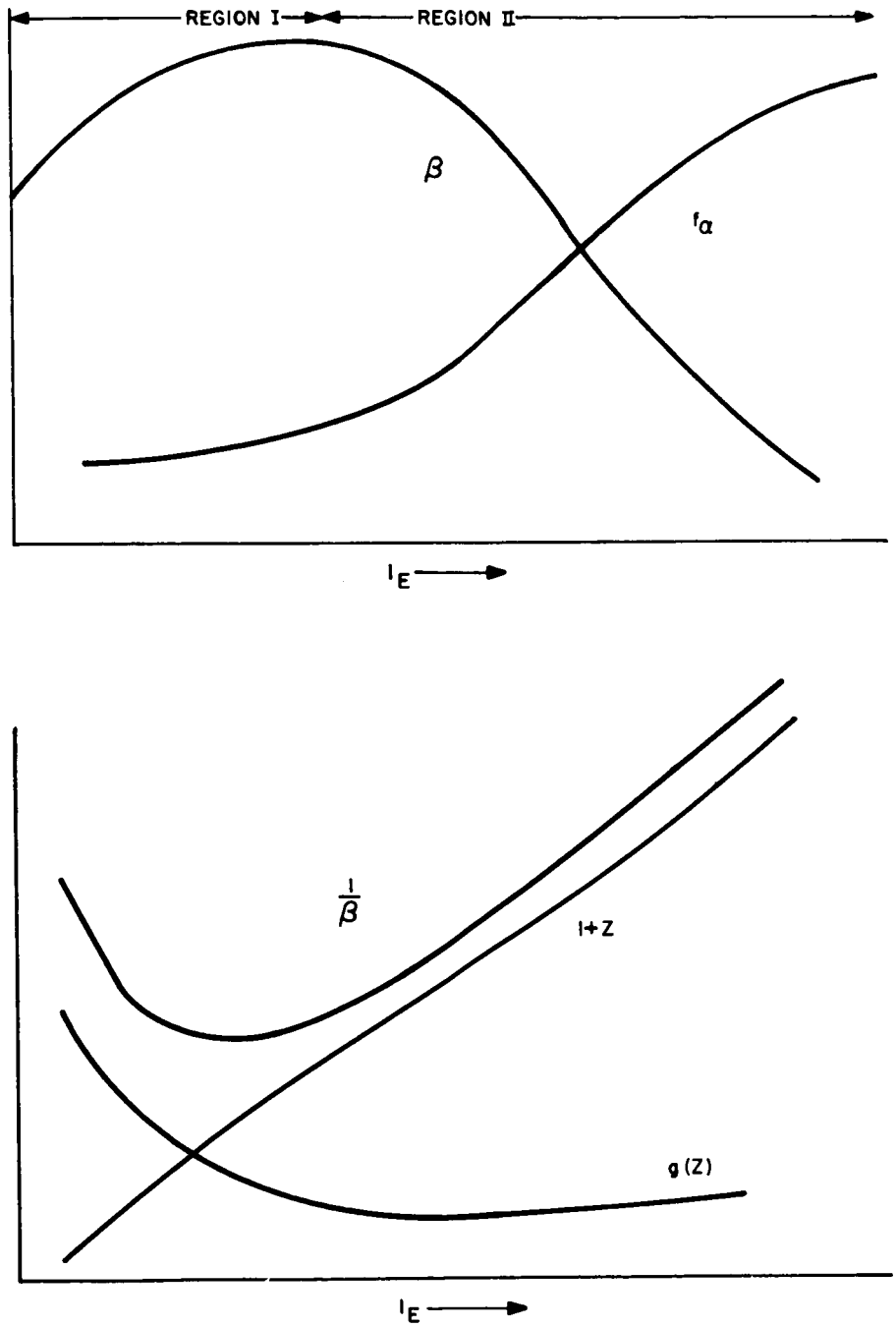

Figure 10. Dependence of Common Emitter Current Gain and Alpha-Cutoff Frequency on Emitter Current

I_E. In region I changes in surface effects (with I_E) will dominate. In region II the electric field set up by the current through the base region diminishes the loss of carriers to the surface, hence reducing the importance of surface effects.

In addition $f_{c\alpha}$, the frequency at which the common base current gain decreases to 0.707 of its low frequency value, can change by an order of magnitude [31, 32] as emitter current is increased. As $f_{c\alpha}$ can be an important factor in assessing and predicting radiation damage its variation must be appropriately evaluated or its effect eliminated from the data.

Operating temperature can also severely affect current gain. [33] This is particularly true for those transistors whose surfaces have not been stabilized so as to fix the surface recombination velocity. [34]

Ionic conduction in the multilayer regions of absorbed water on the surface and other effects can degrade the performance of even inactive transistors. Hence, it is essential that pre-irradiation data be obtained on each device shortly before irradiation and that the temperature be fixed at the same value during irradiation or its temperature dependence evaluated and eliminated from the data.

RADIATION DEPENDENCE OF TERMS OF WEBSTER'S EQUATION

Degradation of β under neutron irradiation has been clearly related by prior studies (24, 35, 22, 36) to lattice defects and the consequent reduction in minority carrier lifetime discussed in the preceding section. In good modern transistors whose surface recombination regions have been "passivated" and where operation is in region II of Figure 1

$$\frac{WA_s}{D_p A_e}\, g(Z)\frac{\partial S}{\partial \varphi} << (1+Z)\frac{W}{L_e}\,\frac{\partial\left(\frac{\sigma_b}{\sigma_e}\right)}{\partial \varphi} << \frac{(1+Z)W^2}{2D}\,\frac{\partial\left(\frac{1}{\tau}\right)}{\varphi}$$

Hence, for constant values of I_E

$$\frac{\partial\left(\frac{1}{\beta}\right)}{\partial \varphi} = \frac{W^2}{2D} \quad \frac{\partial\left(\frac{1}{\tau}\right)}{\partial \varphi}$$

From equation 26

$$\frac{\partial\left(\frac{1}{\beta}\right)}{\partial \varphi} = \frac{W^2}{2D} K$$

Then

$$\frac{1}{\beta} = \frac{1}{\beta_o} + \frac{W^2}{2D} K \varphi$$

Where β_o is the current gain before irradiation, and K is the damage constant for the type of radiation dosage concerned.

APPLICATION OF THE METHOD OF PREDICTING TRANSISTOR DEGRADATION DURING PROTON BOMBARDMENT

The typical irradiation of transistors by neutrons yields data which are fit reasonably well by a linear relation between $1/\beta$ and the neutron flux.

Thus

$$\frac{1}{\beta} = \frac{1}{\beta_o} + \alpha_N \varphi_N = \frac{1}{\beta_o} + \frac{1}{2} \frac{W^2}{D} K_N \varphi_N \qquad (32)$$

The transistor damage constant α_N is simply related to the lifetime damage constant K_N by

$$\alpha_N = \frac{1}{2} \frac{W^2}{D} K_N \quad nvt^{-1} \qquad (33)$$

where W is the base width and D the diffusion constant. If the base width is characterized well by the alpha-cutoff frequency, α_N may be written as

$$\alpha_N = \frac{.2}{f_{c\alpha}} \quad K_N \tag{34}$$

If one now wishes to apply this to a proton irradiation K_N must be modified by introducing the proton damage rate R_{DP} and the neutron damage rate R_{DN} as in equation 28.

The transistor damage constant for use in a proton irradiation is then

$$\alpha_P = \frac{.2}{f_{c\alpha}} \quad \frac{K_N}{R_{DN}} \quad R_{DP} = \frac{\alpha_N}{R_{DN}} \quad R_{DP} \tag{35}$$

If one wishes to use neutron data from a transistor of a type different from that for which the proton effect is being calculated then one must use

$$\alpha_P = \frac{f_{c\alpha}}{f'_{c\alpha}} \quad \frac{\alpha_N}{R_{DN}} \quad R_{DP} \tag{36}$$

Where $f_{c\alpha}$ refers to the transistor for which α_N has been determined and $f'_{c\alpha}$ to that for which α_P is being determined. The ratio of alpha-cutoff frequencies accounts for differences in base widths.

A straightforward application of this method to some of the few silicon transistors for which proton irradiation data exists yields reasonably good agreement as the following examples will show.

Example 1: 2N743, NPN MESA, $f_{c\alpha} \approx$ 400 Mc

Proton irradiation data for this unit is from Hulten[37] who found that a flux of 1.8×10^{12} protons/cm^2 at an energy of 40 Mev reduced β to 85% of its initial value.

The transistor damage constant to be used with the 2N743 is derived from Puttcamp's[38] neutron irradiation of the 2N697, also a mesa NPN unit with $f_{c\alpha} \approx 150$ Mc. From Putcamp's data (average of 4 units)

$$\alpha_N = 1.8 \times 10^{-15} \text{ nvt}^{-1} \text{ and}$$

$$\alpha_P = \frac{150}{400} \cdot \frac{10^3}{460} \alpha_N = 1.5 \times 10^{-15} \text{ per unit proton flux}$$

From this the proton flux necessary to reduce β to $.85\beta_o$ is calculated and found to be

$$\varphi_P \text{ calc} = \frac{\frac{1}{\beta} - \frac{1}{\beta_o}}{\alpha_P} = 2.7 \times 10^{12} \text{ protons/cm}^2 \qquad (37)$$

using average values of $\frac{1}{\beta}$ and $\frac{1}{\beta_o}$ from Hulten. The ratio of calculated to measured fluxes is

$$\frac{\varphi_P \text{ calc}}{\varphi_{p \text{ exp}}} = 1.5$$

Example 2: Hulten's data shows that an average flux of $.7 \times 10^{12}$ protons/cm^2 at 40 Mev is required to reduce β to $.5\,\beta_o$ for 2N859 PNP alloy ($f_{c\alpha} = 14$ Mc). The lifetime damage constant to be used here is derived from the data of Hicks et al.[39] For the 2N495, also a PNP alloy transistor ($f_{c\alpha} \approx 35$ Mc), they obtained $K_N = 3.2 \times 10^{-7}$ nvt^{-1} sec^{-1} (this is actually the reciprocal of the K_N obtained by Hicks). The transistor damage constant for use with protons is

$$\alpha_P = \frac{.2}{14 \times 10^6} \cdot \frac{10^3}{376} (3.2 \times 10^{-7}) = 1.23 \times 10^{-14}$$

per unit proton flux.

Using this one finds

$$\varphi_P \text{ calc} = 1.5 \times 10^{12} \text{ protons/cm}^2$$

$$\frac{\varphi_P \text{ calc}}{\varphi_P \text{ exp}} = 2.2$$

SECTION V

TRANSISTORS IN SATELLITES

INTRODUCTION

A number of silicon transistors have been selected to cover the field of transistor applications in satellites. The list of devices is composed of fourteen npn and three pnp mesa units and three npn diffused junction units which fulfill the function of switches, signal amplifiers and power amplifiers at frequencies and speeds from low to very high. On the basis of process control and life tests, these are believed to be the best silicon transistors in the field. They have been developed primarily to meet the high reliability demands of military and space applications. Most of the transistors are planar units, i.e., they have a thick SiO_2 coating on their active surfaces. This coating acts to stabilize these active surfaces; therefore, it reduces leakage and helps to prevent surface deterioration with consequent degradation of electrical parameters. These surfaces are expected to remain stable during irradiation; thus, one has greater confidence in restricting permanent damage considerations to minority carrier lifetime changes. The devices have been grouped according to fabrication process and electrical parameters and, within a given family, a single base width characterizes the group reasonably well. The members of a given family may differ in frequency response, however, because of modifications in such things as emitter and collector geometry and conductivity. Data on the selected transistors are presented in Table 3.

The expected useful life of these transistors in a satellite whose orbit causes it to be exposed to Van Allen belt protons has been calculated according to methods discussed in previous sections of this report.

TABLE 3

SELECTED SILICON SATELLITE TRANSISTORS

Group	Type	Structure	Gain Bandwidth	Gain	Function
1	2N709	Planar	$f_T > 500$ Mc	20-120	Very High Speed Switch
	2N917	Planar		20-120	Very High Freq. Amplifier
2	2N916	Planar	$200 < f_T < 500$	30-120	High Freq. Amplifier
	2N914	Planar Epitaxial		30-120	High Speed Switch
	2N708	Planar		30-120	High Speed Switch
3	2N718A	Planar	$50 < f_T < 200$	40-120	Medium Freq. Amplifier & Switch
	2N1613	Planar		40-120	Medium Freq. Amplifier & Switch
	2N1893	Planar		40-120	Medium Freq. Amplifier & Switch (H.V.)
	2N910	Planar		40-120	Medium Freq. Amplifier (Small Signal)
4	2N1675	Mesa	$20 < f_T < 50$	25- 50	Low-Med. Freq. Power Amplifier and Switch
	2N930	Planar		100-300	Low Freq. Amplifier (Low Noise)
5	2N560	Mesa	$2 < f_T < 10$	30- 90	Low Speed Switch
	2N657	Mesa			Low Freq. Med. Power Amplifier and Switch
6	2N1485	Diffused Junction	$.5 < f_T < 1.5$	35-100	Low Freq. Med. Current, High Power Amplifier and Switch
	2N2016	Diffused Junction			Low Freq. High Current, High Power Amplifier and Switch
PNP	2N995	Planar Epitaxial	~100	30-140	Med.-High Freq. Amplifier and Switch
	2N869	Planar			Med.-High Freq. Amplifier and Switch
	2N1132	Mesa			Med. Freq. Amplifier & Switch

THE VAN ALLEN FLUX

Maximum proton exposure will occur for an equatorial orbit in the heart of the inner Van Allen belt. Van Allen[40] gives a total omnidirectional flux above 40 Mev of 2×10^4 protons/cm^2-sec. Using the most recent spectrum data of Freden and White[41] and that of Heckman and Armstrong[42] and normalizing to the Van Allen total above 40 Mev the idealized spectrum of Figure 11 is obtained. In applying this spectrum the protons below 1 Mev will be ignored, for the thinnest transistor case will absorb more than 1 Mev protons. The resultant change in the spectrum and secondaries will also be negligible.

CALCULATION OF THE EFFECTS OF VAN ALLEN BELT PROTONS ON SELECTED TRANSISTORS

The total displacement production for a circular equatorial orbit in the most intense portion of the Van Allen belt (at an altitude of approximately 1,200 miles) will be

$$\int R_{DP}(E) \frac{d\varphi_p'(E)}{dE} dE = \bar{R}_{DP} \varphi_p' \tag{38}$$

where φ_p' is the most intense flux rate in the inner Van Allen belt and $\bar{R}dp$ is the weighted average displacement production rate of the proton energy spectrum, $\frac{d\varphi_p'(E)}{dE}$.

Using $R_{DP}(E)$ as given in Figure 5 and the idealized Van Allen belt proton spectrum as given in Figure 11 one finds

$$\bar{R}_{DP}\varphi_p' = 5 \times 10^7 \text{ displacements/cm}^3\text{-sec}$$

Then assuming constant I_E and negligible surface effects

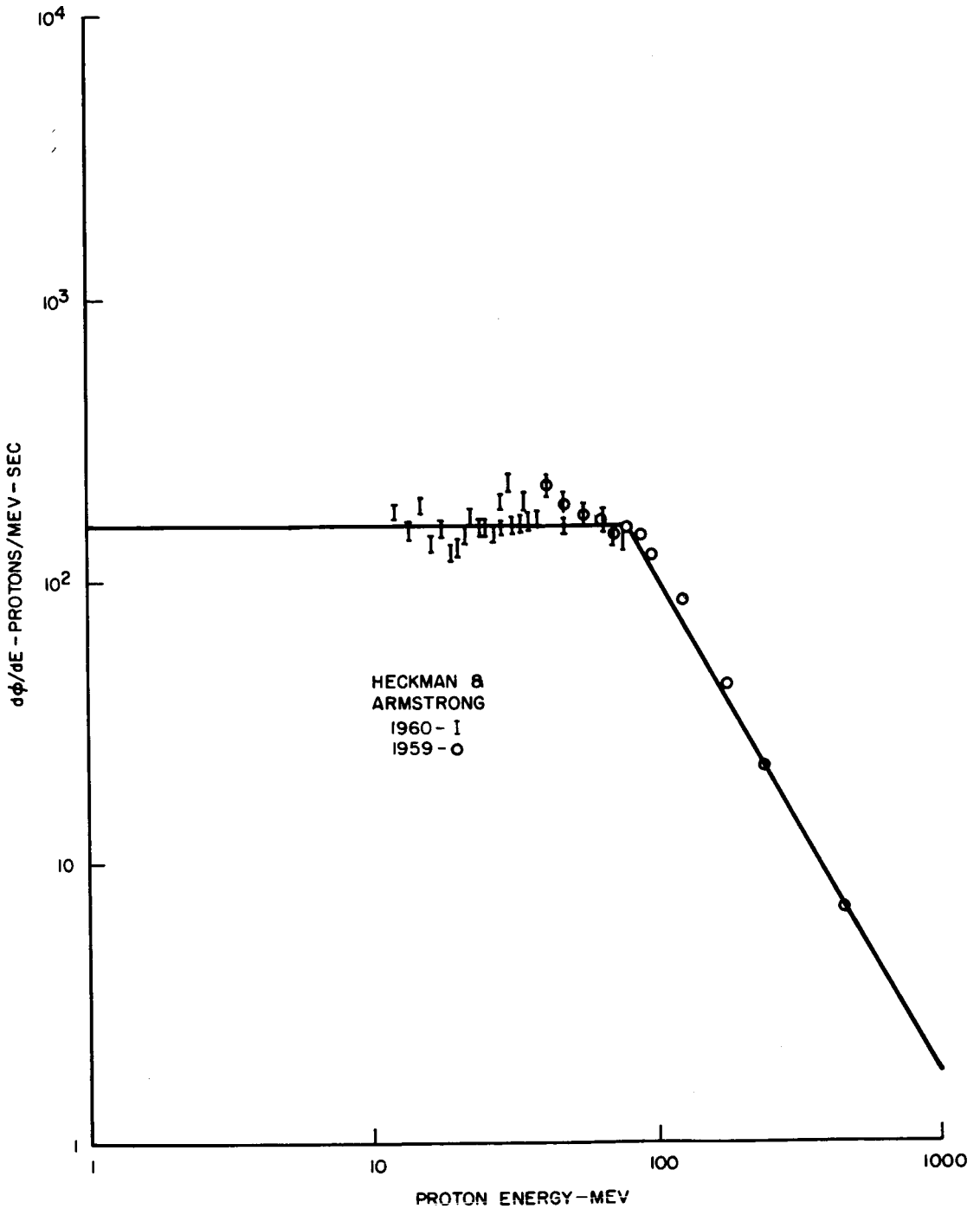

Figure 11. Inner Van Allen Belt Proton Flux Spectrum

$$\frac{1}{\beta} = \frac{SWA_s}{D\,A_e} + \left[\frac{W^2}{2D\,\tau} + \frac{\sigma\,W}{\sigma_e L_e}\right] \tag{39}$$

$$\frac{1}{\tau} = \frac{1}{\tau_o} + K\varphi \tag{40}$$

$$\frac{1}{\beta} = \frac{SWA_s}{D\,A_e} + \frac{\sigma\,W}{\sigma_e L_e} + \frac{W^2}{2D}\left[\frac{1}{\tau_o} + K\varphi\right] \tag{41}$$

$$\frac{1}{\beta} = \frac{1}{\beta_o} + \frac{W^2}{2D}\,K\varphi \tag{42}$$

$$\frac{\beta_o}{\beta} = 1 + \frac{W^2\beta_o}{2D}\,K\varphi \tag{43}$$

For degradation of current gain by 50%

$$\frac{\beta}{\beta_o} = \frac{1}{2} \quad \text{and} \quad \frac{W^2\beta_o}{2D}\,K\varphi_{1/2} = 1 \tag{44}$$

or

$$K\varphi_{1/2} = \frac{2D}{W^2\beta_o} = K\varphi' t_{1/2} \tag{45}$$

whence

$$t_{1/2} = \frac{2D}{W^2\beta_o} \times \frac{1}{K\varphi'} \tag{46}$$

and, substituting K_P from equation 28

$$t_{1/2} = \frac{1}{W^2 \beta_o} \quad x \quad \frac{2DR_{DN}}{k_N} \quad x \quad \frac{1}{\bar{R}_{DP} \varphi'_P} \tag{47}$$

where the factor $1/W^2 \beta_o$ is determined by the particular transistor under consideration and $2DR_{DN}/k$ by the type of material in the base region. Using values of $D_n = 40$ cm^2/sec and $D_p = 10$ cm^2/sec for p and n type materials respectively, the average neutron displacement production rate for the fission spectrum and lifetime damage constants derived from the average values given by Messenger and Spratt[22] one finds for pnp transistors

$$\frac{2 D_p R_{DN}}{K} = \frac{2 \times 10 \times 376}{3.57 \times 10^{-7}} = 2.1 \times 10^{10} \text{ defects}$$

and for npn's

$$\frac{2 D_n R_{DN}}{K} = \frac{2 \times 40 \times 376}{3.12 \times 10^{-7}} = 9.6 \times 10^{10} \text{ defects} \tag{49}$$

From the evaluation of equation (38) one has $R_{DP} \varphi'_p = 5 \times 10^7$ displacements-cm^3 sec for the assumed orbit in the Van Allen belt. Thus for pnp's

$$t_{1/2} = \frac{1}{W^2 \beta_o} \quad x \quad \frac{2.1 \times 10^{10}}{3 \times 10^7}$$

$$t_{1/2} = \frac{700}{\beta_o} \text{ seconds}$$

and for npn's

$$t_{1/2} = \frac{9.6 \times 10^{10}}{3 \times 10^7} \quad x \quad \frac{1}{W^2 \beta_o} = \frac{3200}{W^2 \beta_o} \text{ seconds.}$$

The results of these calculations are shown on Figure 12.

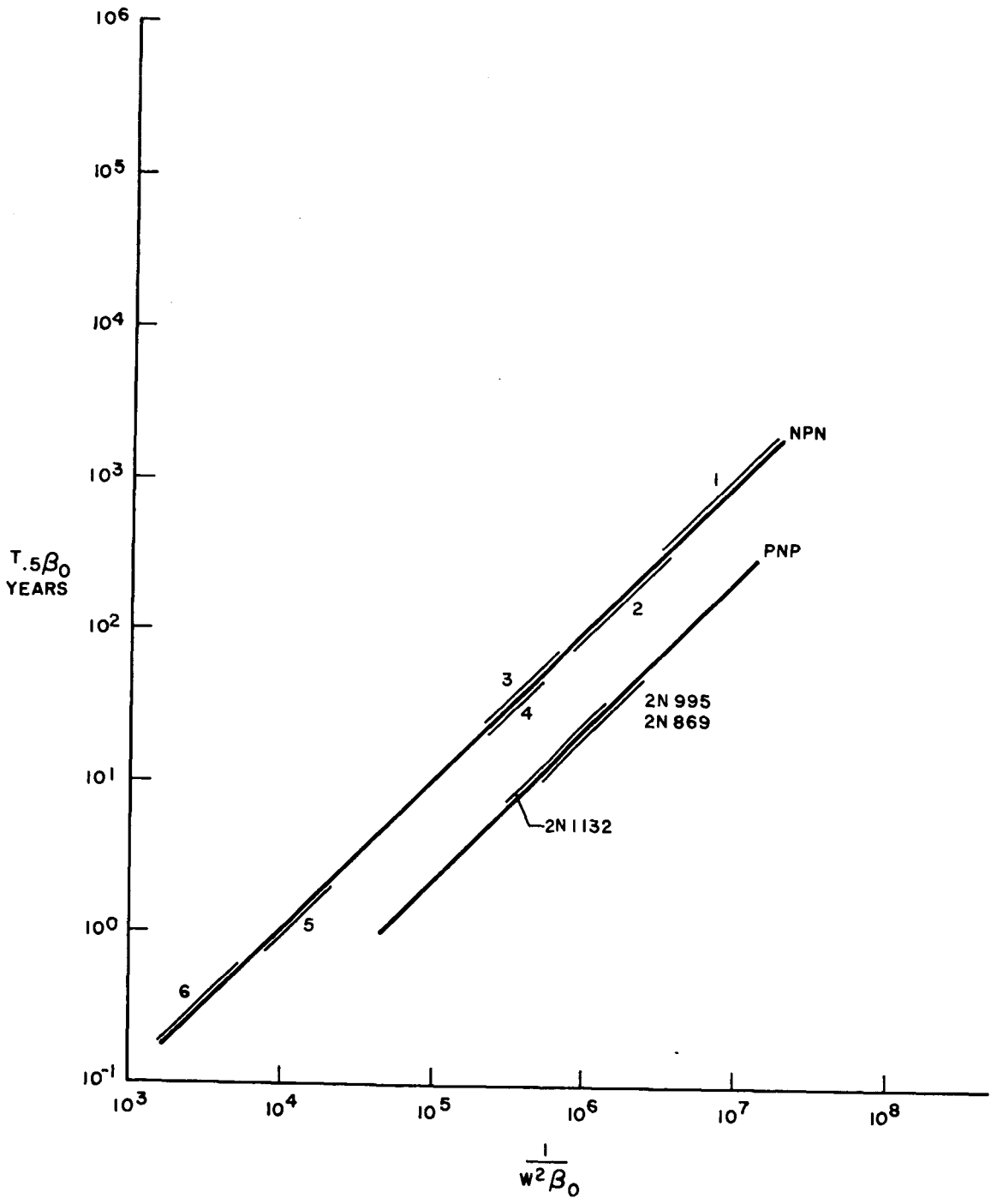

Figure 12. Time in Inner Van Allen Belt for 50% Reduction in Current Gain as a Function of Base Width and Initial Gain

SECTION VI

PROTON INDUCED IONIZATION

INTRODUCTION

Most of the energy which a proton loses in passing through matter is dissipated in the form of ionization and excitation of electrons in the atoms of the target material. In semiconductor material this is ultimately observed as the generation of hole-electron pairs. These excess carriers influence the current flowing in a transistor in several ways. Minority carriers generated in and near the reverse biased collection-base junction will be swept into the collector immediately. This has been called the primary photocurrent. Majority carriers generated in the base may be trapped there by the potential barriers at the emitter and collector junctions and may influence the effective bias at those junctions. The current thus produced is known as the secondary photocurrent.

There are three aspects of the problem of determining the effects on transistors. First, one must determine the energy dissipated by the proton in passing through the material. Second, one must find the number of hole-electron pairs associated with the energy deposition; and finally, one must examine the transistor to find the currents caused by the introduction of excess carriers.

STOPPING POWER

Much work, theoretical and experimental has been done[1, 43, 44] in determining the stopping power, i.e., the energy loss per unit path length in several materials and as a function of particle energy. The stopping power is given by

$$-\frac{dE}{dX} = \frac{2\pi n e^4}{m v^2}\left\{\ln\left[\frac{2 m v^2 W_{max}}{I^2 (1-\beta^2)}\right] - 2\beta^2 - \delta - U\right\} \qquad (50)$$

where: n = density of electrons in stopping substance

m = mass of electron

v = velocity of incident particle

W_{max} = maximum energy transferred to atomic electron by incident particle.

I = mean excitation potential of the atoms in the stopping substance.

β = v/c; c = velocity of light

δ, U = relatively minor corrections for the density and shell effects.

Sternheimer[44] has calculated and tabulated $\frac{1}{\rho}\frac{dE}{dX}$, the energy loss by ionization in Mev - cm^2/gm, for a number of substances. The values for aluminum, corrected for the density of silicon, have been used here. The upper curve in Figure 13 gives the energy loss per cm of proton path in silicon as a function of proton energy.

NUMBER OF CARRIERS LIBERATED

The second part of the problem is to determine the number of carriers liberated by the deposition of a given amount of energy. McKay and McAfee[45] measured the quantity of electrical charge liberated when heavy charged particles passed through germanium and silicon. They found that 3.6 ev were required to create one hole-electron pair in silicon. The number of pairs generated per unit path (or the density of pairs per unit flux) is given by

$$\frac{g}{\varphi} = \frac{dE/dX}{3.6} \tag{51}$$

The lower curve in Figure 13 shows g/φ as a function of proton energy. Obviously, the density of excess carriers is directly proportional to the flux rate.

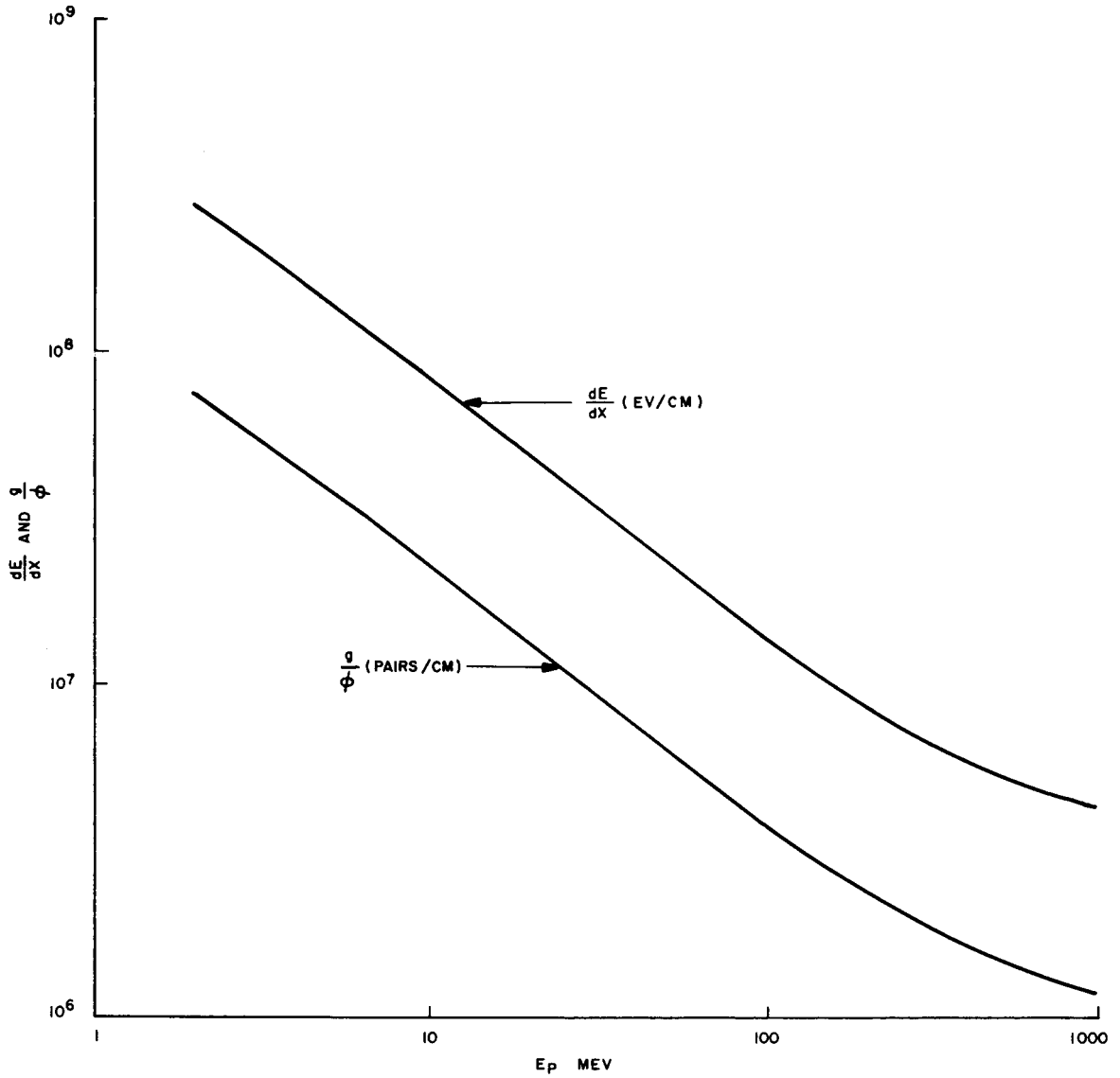

Figure 13. dE/dx and g/φ versus E_p for Silicon

IONIZATION CURRENT

Assuming now that the generated carriers are collected at the device terminals, one finds that the primary ionization current is given by

$$I_i = q \frac{g}{\varphi} \dot{\varphi} V_s \tag{52}$$

where: q = the electronic charge

$\dot{\varphi}$ = the incident particle flux rate (no./cm^2-sec)

V_s = the sensitive volume of the device.

The sensitive volume of the device is the depletion region of the reverse biased collector-base junction and a region extending to one diffusion length from the junction, since carriers generated there will diffuse to the junction. If, as is usually the case, the diffusion length is greater than the base width of the transistor, then the sensitive volume is taken to be the base plus the collector-base depletion region.

The current associated with the radiation generated carriers is thus similar to that portion of the reverse leakage current, I_{co}, due to thermally generated carriers in and near the collector-base junction. The collector current is ordinarily given by

$$I_c = \beta I_B + (\beta + 1) I_{co} \tag{53}$$

If the radiation generated current I_i is included this becomes

$$I_c = \beta I_B + (\beta + 1) I_{co} + (\beta + 1) I_i \tag{54}$$

In the experiment of Hulten, Honaker and Patterson,[46] in which transistors were irradiated by 22 Mev protons at a flux rate of 2.5×10^{10} protons/cm^2-sec, ionization induced currents on the order of several milliamperes were observed. This is several orders of magnitude greater than that calculated from the third term on the right side of equation Using numerical values of $\beta = 50$; $g/\varphi = 1.2 \times 10^{7}$ cm^{-1}; $\dot{\varphi} = 2.5 \times 10^{10}$ cm^{-2} sec^{-1} and $V_s = 7 \times 10^{-6}$ cm^3 (corresponding to a rather old low frequency type of device), this term is approximately .02 ma. Apparently the secondary photocurrent phenomenon is responsible for the large

currents observed. This effect occurs when majority carriers are generated in the base and trapped there by the potential barriers at the junctions. This stored charge effectively changes the emitter base bias. Since the junction current varies exponentially with the bias voltage, large currents may be produced in this manner. The effect is discussed by McKay[47] who noted a quantum yield of 60 and by Keister's group at Boeing[48] which indicated that an increase by a factor of 10^2 over the primary photocurrent might be expected. This is sufficient to give qualitative agreement with the data of Hulten, et al. In a precise calculation one must consider the applied biases as well as the external circuitry since these will affect the currents in the device. However, the present analysis is sufficient to demonstrate that the performance of semiconductor devices exposed to the relatively low proton flux rates encountered in the Van Allen belt and in solar flares will not be significantly affected by ionization currents.

SECTION VII

CONCLUSIONS

1. The rate of production of lattice displacements in silicon has been calculated for proton energies from 1.5 to 180 Mev from Rutherford scattering (below 10 Mev) and from Rutherford plus elastic nuclear scattering (above 10 Mev). Elastic scattering is sufficient to give a good account of the displacement production rate for proton energies up to 100 Mev. Up to 100 Mev this displacement production rate has been found to agree well with the experimentally determined rate of incidence of electrical damage in solar cells. This indicates that the number of electrical defects is directly proportional to the number of lattice displacements. At proton energies above 100 Mev the solar cell damage rate exceeds the displacement production rate calculated from elastic scattering (e.g., by a factor of 2.5 at 180 Mev), indicating that displacements resulting from nuclear reactions are increasingly important at higher energies.

2. Neutron irradiation data has been used in predicting the effects of proton irradiation on transistors and good agreement with experiment has been found. This indicates that the assumptions used in making the prediction, namely that the electrical damage rates are directly proportional to the displacements production rates and that the proton and neutron produced defect clusters are similar in their effects on transistors, are reasonable ones. Thus, the large body of neutron irradiation data may be converted into proton damage information in a rather direct manner.

3. The number of electrical defects associated with transmutated atoms produced by a proton at a given energy has been found to be significantly smaller than that resulting from displacements indicating that the latter is the most important factor in determining permanent device damage in a proton irradiation.

4. Currents generated in transistors as a result of proton induced ionization and electron excitation are unimportant at the flux rate encountered in the Van Allen belt.

SUPPLEMENT

The work discussed in this supplement was performed during the period 1 November 1962 to 4 February 1963 under an extension to contract NAS1-1654. This extension was granted in order that the methods used in the determination of the effects of proton bombardment on silicon devices might be applied to germanium devices.

SECTION VIII

PROTON DAMAGE IN GERMANIUM TRANSISTORS

INTRODUCTION

An attempt was made to extend the method of predicting proton damage in silicon semiconductor devices to include predictions for germanium devices. Since this method has been previously discussed at length, it will only be outlined here. It consists of calculating the displacement production rates of protons and neutrons at various energies and then using these displacement rates to modify, for use in a proton flux, the lifetime damage constants measured in a neutron irradiation experiment. Similar approximations are made regarding cross section data and ionization losses by the primary recoil. Scattering cross sections from p + Cu, n + Cu and n + Zn experiments are used in the absence of p + Ge and n + Ge data. That these are reasonable approximations is indicated by the nuclear optical model which predicts a small rate of change of the differential scattering cross section with atomic mass. The proton displacement calculation, neutron displacement calculation and a comparison of the effects of the two particles on germanium transistors are given in the following sections.

PROTON-INDUCED LATTICE DISPLACEMENTS

The number of lattice displacements per centimeter of proton path has been calculated at incident proton energies of 9.8, 17 and 95 MeV by using the cross section data shown in Figure 14. There exists a rather large void between the 17- and 95-MeV points because there is no data for nuclei sufficiently close to germanium in this interval. The results of the calculation are shown in Figure 15. The points at 1.5 and 5 MeV were calculated from the Rutherford cross section. The points at 9.8, 17 and 95 MeV were calculated from measured total scattering cross sections, which include the effects of both Coulomb and nuclear forces. The dashed line is an extrapolation of the Rutherford scattering.

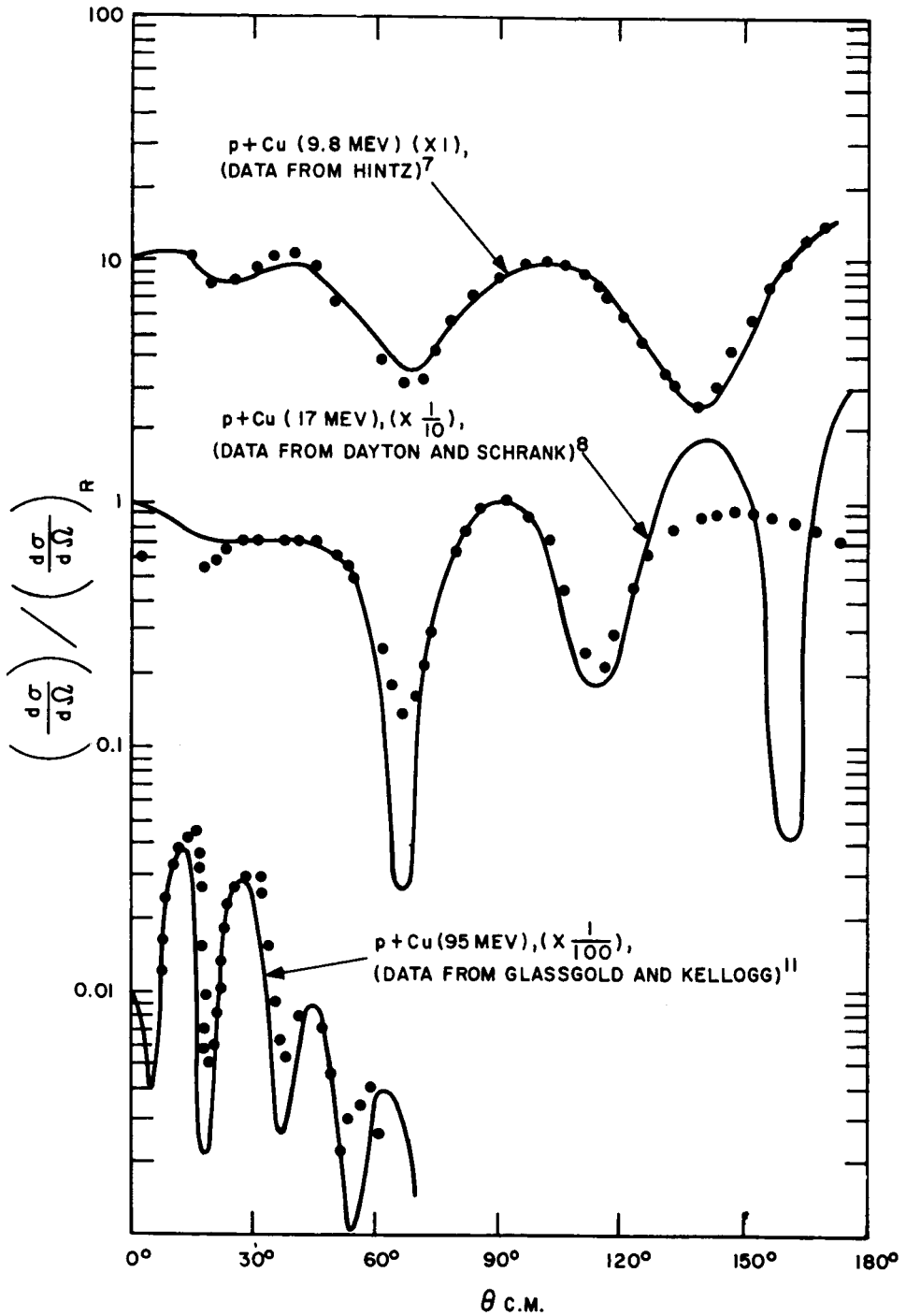

Figure 14. The Ratio of the Measured Elastic Cross Section, $d\sigma/d\Omega$, to the Rutherford Cross Section ($d\sigma/d\Omega$), for Protons Scattered by Copper

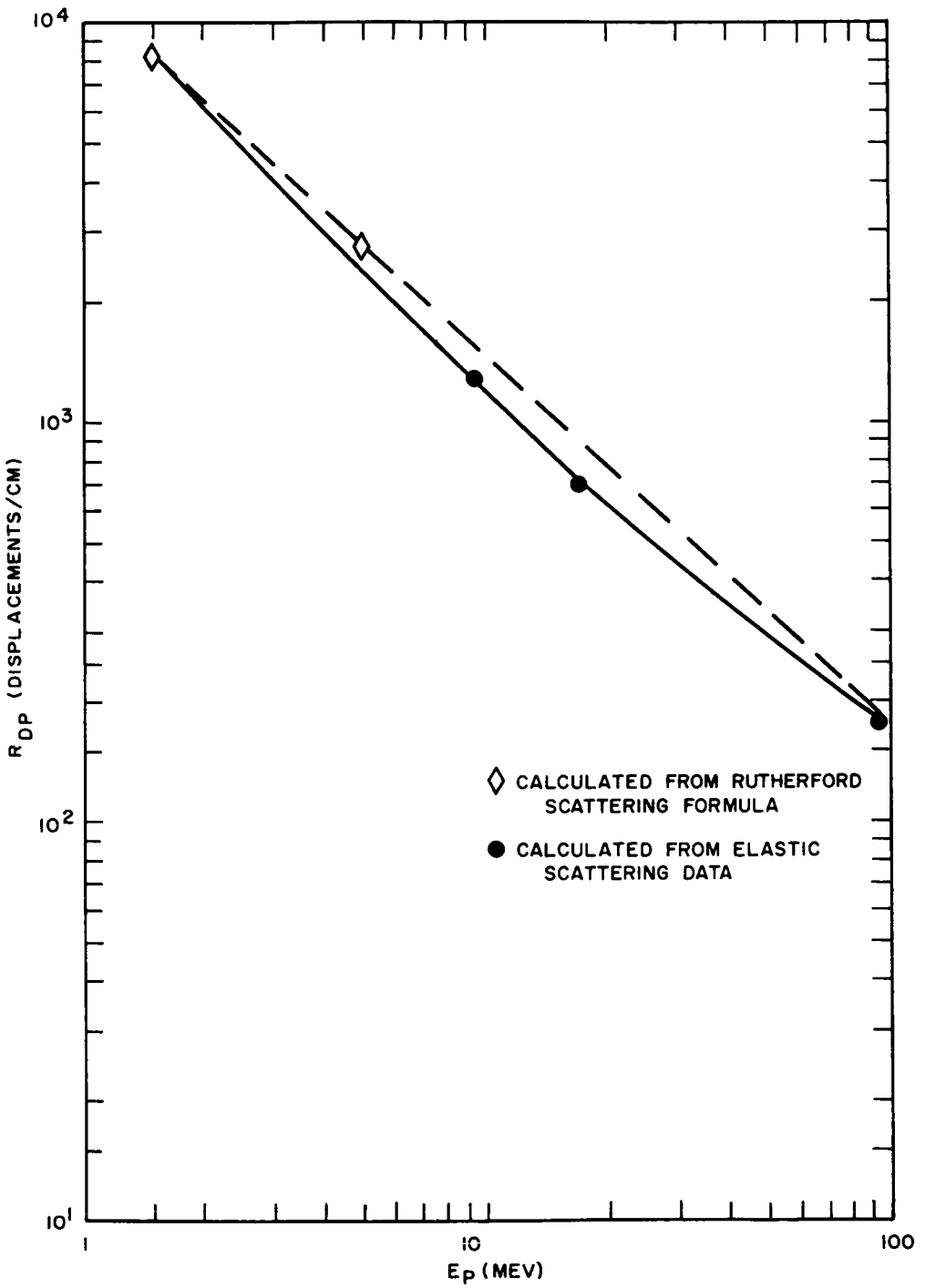

Figure 15. The Number of Lattice Displacements R_{DP}, per Centimeter Along the Track of a Proton in Germanium

It is interesting to compare the curve calculated for germanium with that calculated for silicon (see Section I, Figure 5, page 17). The most significant difference occurs in the energy interval from 10 to 40 MeV. The displacement rate in silicon is significantly greater than that expected from simple Rutherford scattering, while in germanium the displacement rate is actually less than would be expected from Rutherford scattering. This is consistent with the optical model prediction of a decrease in the amplitude of the diffraction pattern with increasing atomic weight.

The displacement rate calculated from the elastic scattering of 95-MeV protons by silicon is apparently too low by a factor of 2. This is probably indicative of the importance of inelastic processes, which generate a secondary displacement-producing flux. One may assume that these processes have a comparable importance in germanium, i.e., that they account for as many displacements at 95 MeV as do the elastic processes. The dashed curve in Figure 16 indicates the approximate displacement rate, including the contribution of inelastic processes.

In all the displacement calculations the assumption has been made that none of the primary recoil energy was expended in electron excitation. Because the germanium atom is more massive, this approximation is better justified for germanium than for silicon.

NEUTRON-INDUCED LATTICE DISPLACEMENTS

In this section R_{DN}, the number of displaced germanium atoms per centimeter of neutron path, will be computed from the expression

$$R_{DN} = \frac{0.47\ n_{Ge}}{E_D} \bar{T}\ \sigma_{Te} \tag{55}$$

where $\bar{T}$ is the average energy imparted to a primary recoil germanium atom by a neutron of given energy, and σ_{Te} is the total elastic scattering cross section.

As pointed out previously, there is no angular distribution data for neutrons elastically scattered by germanium nuclei and so data from the n + Cu and n + Zn

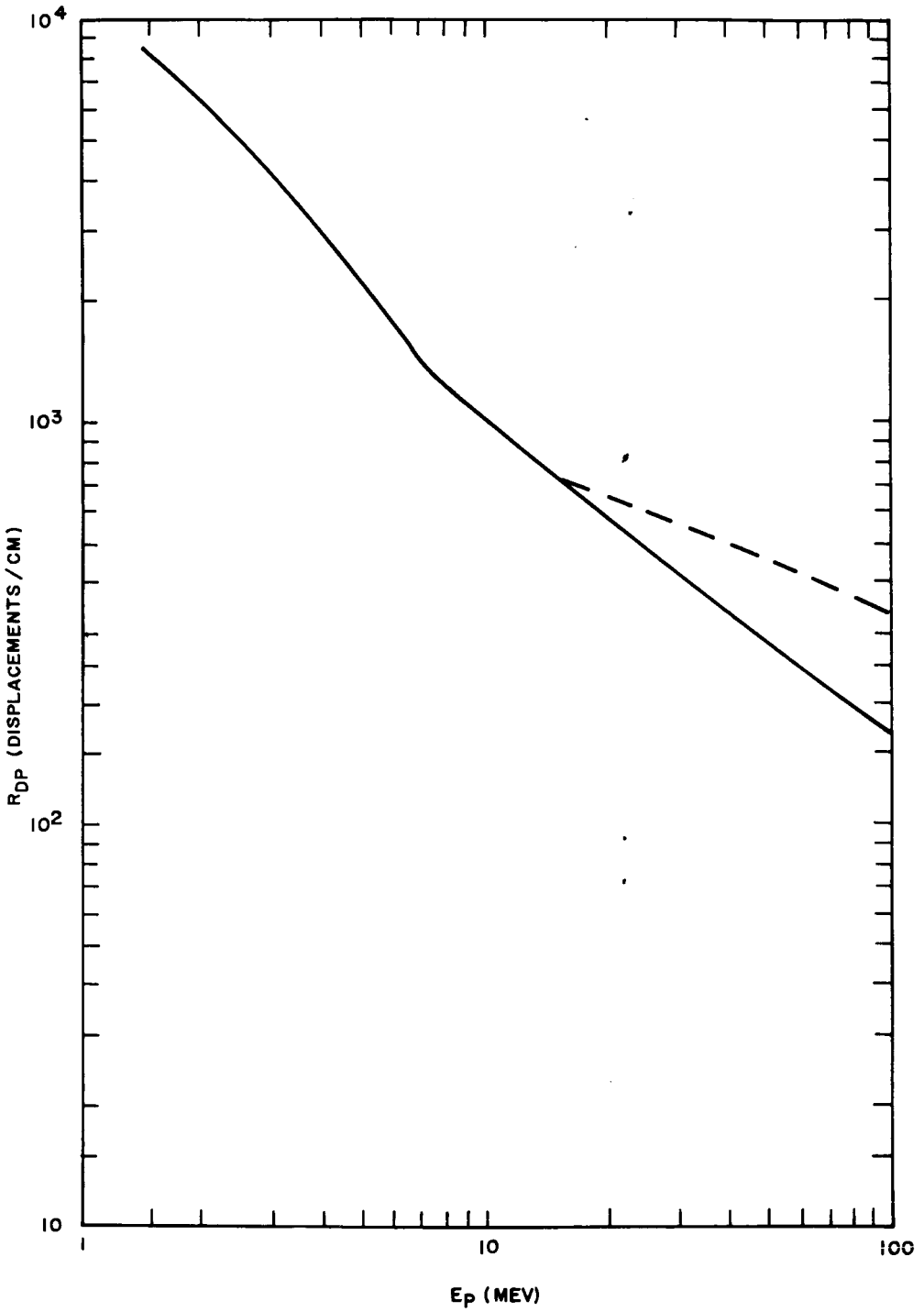

Figure 16. Possible Effect of Inelastic Processes at High Incident Proton Energies

interactions must be used to calculate $\overline{T}$. This has been done by Binder.[17] His results are shown as the solid line in Figure 17. The dashed curve is an approximate extrapolation whose shape is unimportant since only about 5% of the neutrons in the fission spectrum have energies greater than 5 MeV.

Total elastic scattering cross section data were obtained by subtracting the non-elastic components for zinc from the total cross sections for germanium.

$\overline{R}_{DN}$ has been computed from Equation 55 for neutron energies from 0 to 10 MeV. These calculations are plotted in Figure 18. The weighted average displacement rate for the neutron spectrum in a pulsed TRIGA reactor, as reported by DOFL, is shown as R_{DN}. The approximate constancy of R_{DN} between 1.8 and 4.8 MeV, which Binder used to interpret the experiment of Ruby, Schupp and Wolley,[18] is apparent in Figure 18.

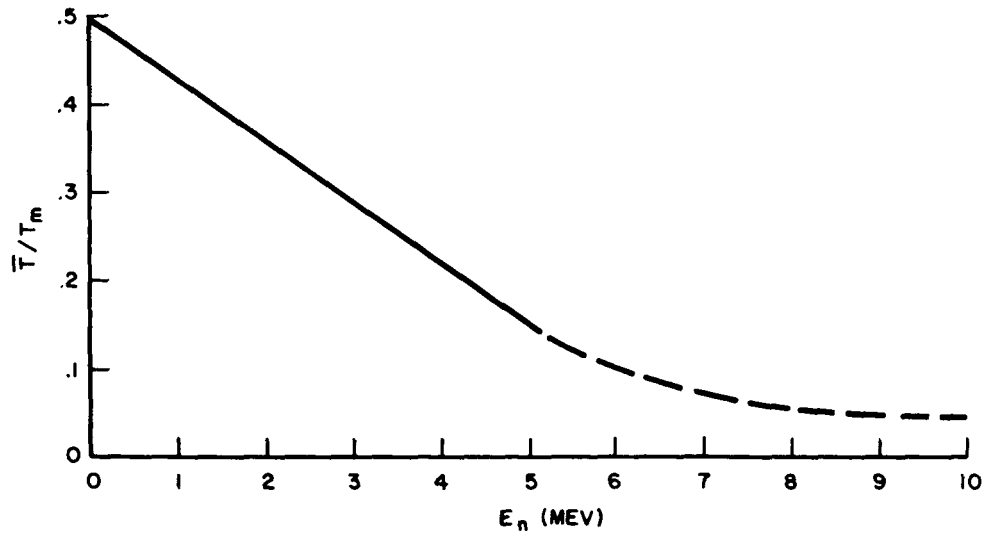

Figure 17. The Ratio of the Average Energy to the Maximum Energy Imparted to Recoil Germanium Atoms Displaced by Neutrons of Energy E_n

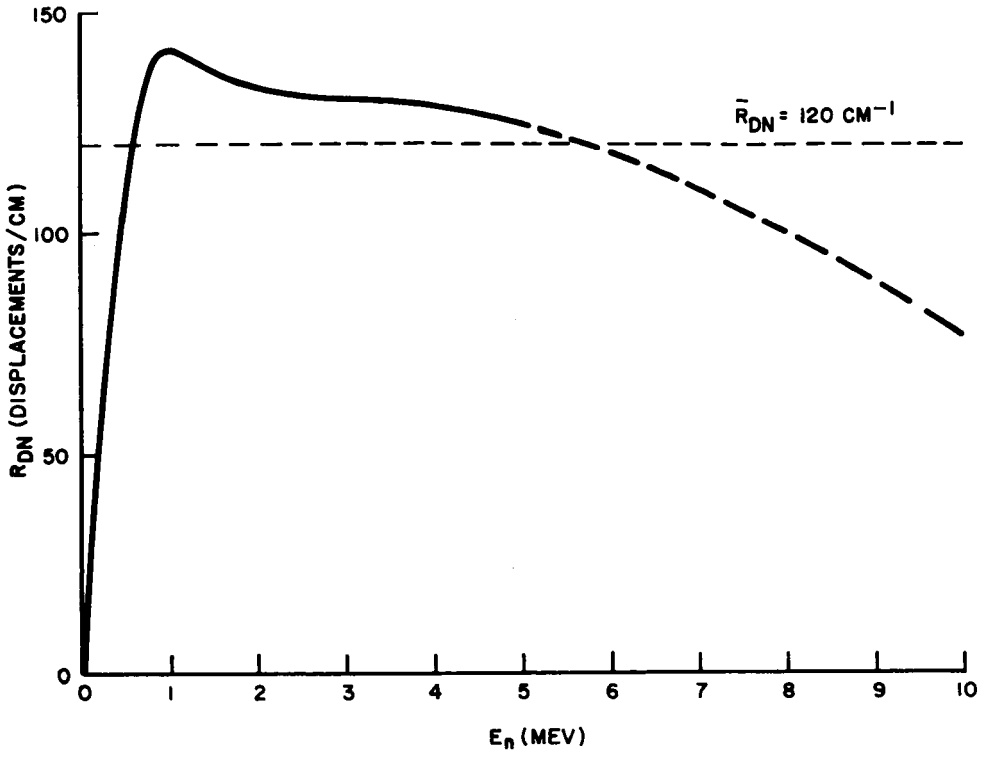

Figure 18. The Number of Lattice Displacements R_{DN}, per Centimeter Along the Track of a Neutron in Germanium

COMPARISON OF THE EFFECTS OF PROTON AND NEUTRON BOMBARDMENT ON GERMANIUM TRANSISTORS

The proton irradiation data (degradation of transistor current gain during 40-MeV protons radiation) of interest are those of Hulten and Honaker.[37] Their results for germanium pnp transistors are summarized in Table 4. The lifetime damage constants have been calculated from

$$k = \left(\frac{1}{\beta} - \frac{1}{\beta_0}\right) \frac{f_{c\alpha}}{.2} \frac{1}{\varphi} \tag{56}$$

The change in the effective base width described by Easley and Dooley[51] has been neglected here. The resultant error introduced is not serious inasmuch as the data in Reference[51] indicate that rather large fluxes (on the order of 10^{14} nvt or more) are required to give a significant effect. Of the devices in Table 4, only the 2N224 shows an appreciable change in $f_{c\alpha}$. The small changes in the other

TABLE 4

40-MeV PROTON IRRADIATION OF GERMANIUM
pnp ALLOY TRANSISTOR

Type No.	$f_{\alpha\alpha}$ (Mc)		β		% Change	k_p
	Initial	Final	Initial	Final		
2N224	1.1	0.72	143	17.3	-88	1.6×10^{-7}
2N526	4.2	3.5	75.5	16.3	-79	5.6×10^{-7}
2N1303	9.8	9.7	95	70	-26	1.0×10^{-7}
2N1305	7.7	7.1	90	31	-66	4.5×10^{-7}
Total Proton Flux = 1.8×10^2 particles/cm^2 Tabulated Values are on Averages of 6 or 8 Units						

three units indicate that there has been little or no change in effective base width. The proton irradiation data of the NASA group may be compared to the neutron irradiation of a group of pnp germanium alloy transistors reported by DOFL[38]. These are summarized in Table 5. In order for comparisons to be made between the proton and neutron irradiation data, the lifetime damage constant obtained from the neutron experiments must be modified in the manner previously outlined. The calculated damage constant is

$$k_P = \frac{R_{DP}}{R_{DN}} k_N = \frac{360}{120} (.5 \times 10^{-7}) = 1.5 \times 10^{-7}$$

where R_{DP} is taken from Figure 15 at E_p = 40 MeV, and R_{DN} is the average displacement rate for TRIGA neutrons (Figure 18).

Comparisons of the calculated proton damage constant with the measured values given in Table 4 show good agreement for the 2N224 and 2N1303, but rather poor agreement for the 2N526 and 2N1305. However, one should probably not expect really good agreement in light of the considerable spread that exists in the proton

TABLE 5

FISSION NEUTRON IRRADIATION OF GERMANIUM
pnp ALLOY TRANSISTORS

Type No.	$f_{c\alpha}$	β		% Change	ϕ_N	k_N
	Nominal (Mc)				(nvt)	
2N139	7.5	51.9	28.3	-43	1×10^{13}	$.59 \times 10^{-7}$
2N218	6.8	43.5	38.4	-12	3.8×10^{12}	$.27 \times 10^{-7}$
2N219	10.0	62.1	51.0	-15	2.8×10^{12}	$.63 \times 10^{-7}$
Tabulated Values are Averages of 10 Units						k_N (average) $= 0.5 \times 10^{-7}$

irradiation data. This spread is particularly evident in the damage constants for the 2N1303 and 2N1305. These transistors are nearly identical, both being improved versions of the earlier 2N404. It is not apparent why there should be such a large spread in damage constants measured under apparently identical conditions.

CONCLUSIONS

After this analysis of germanium transistor damage, it may be concluded that, as in the case of silicon transistors, the use of suitably modified neutron irradiation data is a reasonable approximation which yields useful information about the effects of proton irradiation on transistors.

REFERENCES

1. See, for example, "The Atomic Nucleus" by R. D. Evans, McGraw-Hill, N. Y. (1955) p. 411
2. G. H. Kinchin and R. S. Pease, Rept. Progr. In Physics. 18, 1 (1955).
3. W. A. Harrison and F. Seitz, Phys. Rev. 98, 1530A (1955).
4. W. S. Snyder and J. Neufeld, Phys. Rev. 97, 1636 (1955); IBID 99,1326 (1955).
5. Complex nuclear potentials were considered by H. Bethe, Phys. Rev. 57, 1125 (1940) and R. Serber, Phys. Rev. 72,1114 (1947). They were used to explain high-energy (90 Mev) neutron scattering by Fernbach Serber and Taylor, Phys. Rev. 78, 1352 (1949). The model has been much refined, by replacing the original square wells with a Saxon-Woods Potential (R. D. Woods and D. S. Saxon, Phys. Rev. 95,577 (1954) and by the inclusion of spin-orbit terms. Some excellent examples of the agreement between the model and experiment are shown by S. Fernbach, Rev. Modern Phys. 30,414 (1958).
6. F. Seitz and J. S. Koehler, Solid State Physics, (Ed. by F. Seitz and D. Turnbull) Academic Press, N. Y. 1956, Vol. 2, p. 307.
7. N. Hintz, Phys. Rev. 106,1201 (1957).
8. I. E. Dayton and G. Schrank, Phys. Rev. 101, 1358 (1956).
9. A. E. Glassgold, Rev. Modern Phys. 30,419 (1958).
10. Gerstein, Niederer and Strauch, Phys. Rev. 108,427 (1957).
11. A. E. Glassgold and P. J. Kellogg, Phys. Rev. 109,1291 (1958).
12. N. Hintz, Bull. Am. Phys. Soc. Ser II, 2, 14 (1957).
13. Johansson, Svanberg and Hodgson, Ark. Fys. (Sweden) 19 541 (1961).
14. Matsuda, Nagahara, Oda, Yamamuro and Kobayashi, Nuclear Physics 27, 1 (1961).
15. G. Bemski, J. Applied Physics 30,1195 (1959).
16. G. D. Watkins and J. W. Corbett, Phys. Rev. 121,1001 (1961).
17. Daniel Binder, Phys. Rev. 122, 1147 (1961).
18. S. T. Ruby, F. D. Schupp, and E. D. Wolley, Phys. Rev. 111, 1493 (1958).
19. B. E. Watt, Phys. Rev. 87, 1037 (1953).
20. Richard Stephenson, "Introduction to Nuclear Engineering", 2nd Ed. p. 228, McGraw-Hill, 1958.

21. W. Shockley and W. T. Read, Phys. Rev. 87, 835 (1952).

22. G. C. Messenger and J. P. Spratt, Proc. IRE, 46, 1038 (1958).

23. P. Rappaport, Phys. Rev. 94, 1409 (A) (1954).

24. J. J. Loferski and P. Rappaport, Phys. Rev. 98, 1861 (1955).

25. P. Rappaport and J. J. Loferski, Phys. Rev. 100, 126 (A) (1955).

26. For example see Section 18 of Handbook of Semiconductor Electronics, Hunter, McGraw-Hill, N. Y. 1962.

27. Proc. IRE, Vol. 44, p. 1542 - 1561, Nov. 1956.

28. J. P. McKelvey, R. L. Longini and T. P. Brady, Phys. Rev. V 123,p. 51 - 57, July 1, 1961.

29. T. P. Brody, Proc. IRE, Letter to the Editor, V 50,No. 6 June 1962,p. 1524.

30. W. M. Webster, Proc. IRE 42, 914, 1954.

31. E. S. Rittner, Phys. Rev. 94, 1151, 1954.

32. C. T. Kirk, Jr., IRE Transactions on Electron Devices,ED-9 #2,(March 1962) p. 165 - 174)

33. C. T. Sah, IRE Transactions on Electron Devices ED-9 #1 (Jan. 1962) p. 94-108;See particularly Figure 11.

34. H. R. Wilson, Semiconductor Products,June 1962,p. 25.

35. J. J. Loferski, J. Appl, Phys. 29 (Jan. 1958).

36. J. W. Easley and J. A. Dooley, J. Appl. Phys. 31, 1024 (June 1960).

37. W. C. Hulten, Symposium, Society of Aerospace Material and Process Engineers, St. Louis, Mo., May 7, 1962.

38. Robert Puttcamp, DOFL, TR-975, 27 Nov. 1961.

39. D. A. Hicks, D. V. Kelly, J. B. Robison, R. K. Durkee, J. R. Orr, B. M. Clarke, Boeing Airplane Co., D 5-2880, 1 Dec. 1958.

40. J. Van Allen, "Origin and Nature of Geomagnetically Trapped Radiation," Proceedings of the First International Space Science Symposium, Jan. 1960.

41. S. C. Freden and R. S. White, Jrnl. of Geophysical Research,Vol. 67, p. 25, 1962.

42. Harry H. Heckman and Alice H. Armstrong, J. Geophys. Research,67, 1255 (1962).

43. Hans A. Bethe and Julius Ashkin, Experimental Nuclear Physics, Vol. 1, p. 166, (1953).

44. R. M. Sternheimer, Phys. Rev. 115, 137 (1959).

45. K. G. McKay and K. B. McAfee, Phys. Rev. 91, 1079 (1953).

46. W. C. Hulten, W. C. Honaker, and John L. Patterson, NASA TN D-718, April 1961.

47. K. G. McKay, Phys. Rev. 84, 833 (1951).

48. Boeing Airplane Co. Report D2 - 9878, Jan. 1962.

49. D.J. Hughes and R.S. Carter, Brookhaven National Laboratory Report BNL-400.

50. D.J. Hughes and R.B. Schwartz, "Neutron Cross Sections", Brookhaven National Laboratory Report BNL-325.

51. J.W. Easley and J.A. Dooley, J. Appl. Phys. 31, 1024 (1960)

NASA-Langley, 1964 CR-40